

1-6-2022

## Applications of nano-zeolite in wastewater treatment: An overview

Rehab O, Abdel Rahman  
*Atomic Energy Authority of Egypt, alaarehab@yahoo.com*

Ahmed M. El-Kamash  
*Atomic Energy Authority of Egypt, kamash20@yahoo.com*

Yung-Tse Hung  
*Cleveland State University, y.hung@csuohio.edu*

Follow this and additional works at: [https://engagedscholarship.csuohio.edu/encee\\_facpub](https://engagedscholarship.csuohio.edu/encee_facpub)

 Part of the [Civil and Environmental Engineering Commons](#)

[How does access to this work benefit you? Let us know!](#)

---

### Original Citation

Rahman, R.O.A.; El-Kamash, A.M.; Hung, Y.-T. Applications of Nano-Zeolite in Wastewater Treatment: An Overview. *Water* 2022, 14, 137. <https://doi.org/10.3390/w14020137>

This Article is brought to you for free and open access by the Civil and Environmental Engineering at EngagedScholarship@CSU. It has been accepted for inclusion in Civil and Environmental Engineering Faculty Publications by an authorized administrator of EngagedScholarship@CSU. For more information, please contact [library.es@csuohio.edu](mailto:library.es@csuohio.edu).

## Review

# Applications of Nano-Zeolite in Wastewater Treatment: An Overview

Rehab O. Abdel Rahman <sup>1,\*</sup> , Ahmed M. El-Kamash <sup>1</sup> and Yung-Tse Hung <sup>2</sup> 

<sup>1</sup> Hot Laboratory Center, Atomic Energy Authority of Egypt, Cairo P.O. Box 13759, Egypt; kamash20@yahoo.com

<sup>2</sup> Department of Civil and Environmental Engineering, Cleveland State University, Cleveland, OH 44115, USA; Y.HUNG@csuohio.edu

\* Correspondence: alaarehab@yahoo.com; Tel.: +20-010-614-044-62

**Abstract:** Nano-zeolite is an innovative class of materials that received recognition for its potential use in water and tertiary wastewater treatment. These applications include ion-exchange/sorption, photo-degradation, and membrane separation. The aim of this work is to summarize and analyze the current knowledge about the utilization of nano-zeolite in these applications, identify the gaps in this field, and highlight the challenges that face the wide scale applications of these materials. Within this context, an introduction to water quality, water and wastewater treatment, utilization of zeolite in contaminant removal from water was addressed and linked to its structure and the advances in zeolite preparation techniques were overviewed. To have insights into the trends of the scientific interest in this field, an in-depth analysis of the variation in annual research distribution over the last decade was performed for each application. This analysis covered the research that addressed the potential use of both zeolites and nano-zeolites. For each application, the characterization, experimental testing schemes, and theoretical analysis methodologies were overviewed. The results of the most advanced research were collected, summarized, and analyzed to allow an easy visualization and comparison of these research results. Finally, the gaps and challenges that face these applications are concluded.

**Keywords:** sorption/ion exchange; photo-catalytic degradation; membrane separation; characterization; models



**Citation:** Rahman, R.O.A.; El-Kamash, A.M.; Hung, Y.-T. Applications of Nano-Zeolite in Wastewater Treatment: An Overview. *Water* **2022**, *14*, 137. <https://doi.org/10.3390/w14020137>

Academic Editor: Carmen Teodosiu

Received: 19 December 2021

Accepted: 3 January 2022

Published: 6 January 2022

**Publisher's Note:** MDPI stays neutral with regard to jurisdictional claims in published maps and institutional affiliations.



**Copyright:** © 2022 by the authors. Licensee MDPI, Basel, Switzerland. This article is an open access article distributed under the terms and conditions of the Creative Commons Attribution (CC BY) license (<https://creativecommons.org/licenses/by/4.0/>).

## 1. Introduction

The sustainability of human life is very much dependent on the availability of clean water not only for personal uses, but also to support the agricultural and various industrial activities. On one hand, the provision of clean water and sanitation (Goal 6) can be considered as a driving force to achieve zero hunger (Goal 2), good health and well-being (Goal 3), decent work and economical growth (Goal 8), and industry, innovation, and infrastructure (Goal 9). On the other hand, placing controls on wastewater and preventing this pollution source from entering the geosphere and biosphere is the driving force to ensure sustainable cities and communities (Goal 11), and life below water (Goal 14) and on earth (Goal 15), which requires partnerships for the goals (Goal 17). Subsequently, aspects related to water quality and the wastewaters management were addressed in the Sustainable Development Goals (SDG) 6 [1]. This recognition for the importance of maintaining the water quality and having efficient and reliable wastewater management system led to the consideration of the wastewaters effluents as biogas resource and an alternative source for potable water [2]. Increased research efforts were directed to improve the treatment performance of the biological, chemical, and physical processes that are used in the primary, secondary, and tertiary treatment of these effluents to meet stringent regulatory requirements on the quality of the treated wastewater. An overview on these requirements is found elsewhere [2]. Tertiary treatment aims to remove persistence organic

contaminants and heavy metals from the effluents generated from the secondary treatment using advanced wastewater treatment technologies [2].

Zeolites, a class of materials, are well known for their wide applications in water and tertiary wastewater treatment, where different types of zeolites are used in filtration, ion exchange, adsorption, photo-catalytic degradation, and membrane separation technologies. These wide applications were designed based on inherent zeolite properties, such as the high ion exchange capacity, large specific surface area, high thermal stability, and lattice stability. The three-dimensional porous crystalline structure of zeolites is responsible for the development of these properties, where the primary building units (PBU) of silicon or alumina tetrahedra ( $\text{TO}_4$  where  $T = \text{Si}$  or  $\text{Al}$ , Figure 1a) are linked to form secondary building units (SBU) of different numbers of PBU, e.g., four, five, . . . etc., that encompass channels and cavities. Figure 2b illustrates the configuration of SBU formed of five tetrahedral rings. The structure accommodates exchangeable charge compensating cations ( $M_b^n$ ), and molecules ( $A_b$ ), e.g., water, salts and can be described using these formulas [3,4]:

$$x_1 M_1^{n_1+}; x_2 M_2^{n_2+}; \left[ (y_1 T_1; y_1 T_1 \dots) O_{2(y_1+y_2+\dots)} \right]^{x-} z_1 A_1; z_2 A_2 \dots \quad (1)$$

$$M_{\frac{a}{n}} \cdot (\text{Al}_2\text{O}_3)_a \cdot (\text{SiO}_2)_b \cdot w\text{H}_2\text{O} \quad (2)$$

Zeolites could be classified based on the ratio of silicon to alumina in PBU, i.e.,  $b/a$ , into high silica ( $b/a > 5$ ), intermediate silica ( $2 < b/a \leq 5$ ), and low silica ( $2 \geq b/a$ ). Zeolites of low and intermediate silica have good electrostatic fields in the cavities which support their uses in the sorption of polar molecules. High silica zeolites are characterized by their hydrophobicity, which support their uses in micro-pollutants removal from industrial wastewater effluents, e.g., personal care products and pharmaceutical. The ability of the PBU to form different configurations of the SBU leads to the formation of hundreds of frameworks of natural and synthetic zeolite and zeotype. The structure of Mordeinite (MOR), as an example of five rings' intermediate silica zeolite ( $b/a = 5$ ), is illustrated in Figure 1c, where the structure accommodates sodium atoms as charge compensating cations and encompasses large cavities and channels.

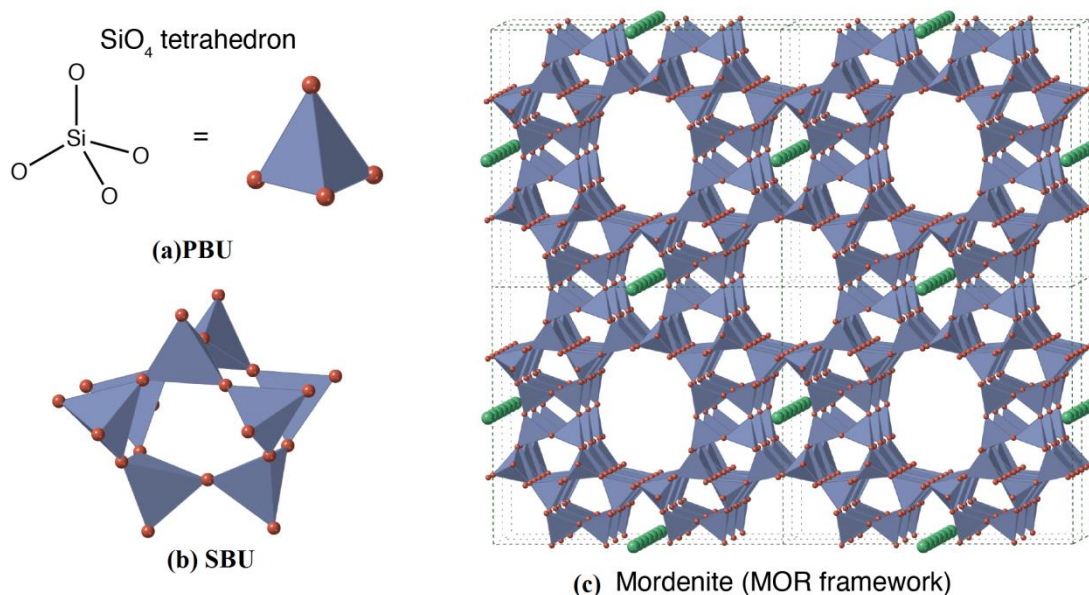


**Figure 1.** The structure of zeolite (a) primary building unit, (b) secondary building unit, (c) Mordeinite framework accommodating  $\text{Na}^+$  cations (green atoms) (copy righted François-Xavier Coudert, wikimedia, [https://commons.wikimedia.org/wiki/File:Zeolite\\_structure\\_as\\_an\\_assembly\\_of\\_tetrahedra.png](https://commons.wikimedia.org/wiki/File:Zeolite_structure_as_an_assembly_of_tetrahedra.png)) (15 October 2021).

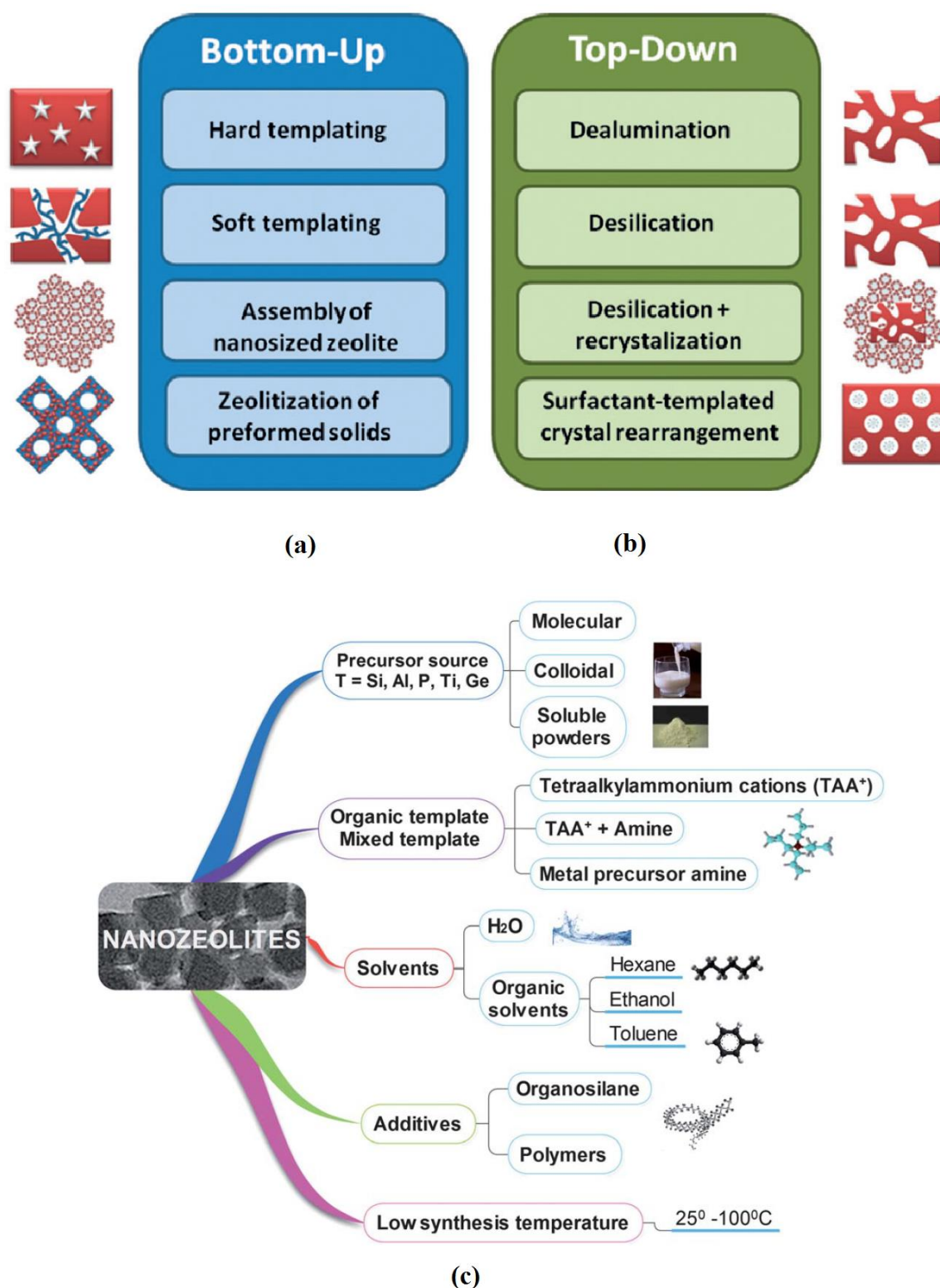


**Figure 2.** Zeolite preparation (a) Hierarchical zeolite bottom-up technique, (b) Hierarchical zeolite top-down techniques (Reprinted with permission from [22] 2021) (c) Factors that affect the properties of the nano-zeolites. (Reprinted with permission from [24]).

Natural zeolites are formed in different geological environments. They are sub-classified as hydrothermal and sedimentary zeolites; the latter are found in lake, ash ponds, and marine sediments and in alkaline deserts [4,5]. Natural zeolite minerals are

usually categorized into families of specified crystalline structure that include different minerals. For instance, the Chabazite (CHA) group, an intermediate silica zeolite composed of six-cyclic rings, has a rhombohedral shape and includes several minerals e.g., Chabazite, willhendersonite, Gmelinite, ... etc. [4,6]. In particular, CHA and Clinoptilolite (CLP) are known for their wide scale application in water treatment, where they are used to remove  $\text{NH}_3$ , Fe, and Mn from surface water, As and Cu from contaminated water, and F from groundwater. These applications are limited for fixed bed operation. In addition, for applications that need the enforcement of quality requirements on the purity and uniformity of the ion-exchanger/sorbent, the importance of synthetic zeolite comes to the surface, where the lattice structure, pore sizes, rings, and compensating ions are optimized by controlling the synthetic conditions, e.g., Si/Al content, use of templates, temperature, pressure, reagent solutions composition and pH, activation process, and ageing conditions [4,7].

Synthetic zeolites are usually prepared via the hydro/solvo-thermal method, where the synthesis system composes of sources for the structural elements, i.e., Al, Si, the mineralizer, e.g., source for  $\text{OH}^-$  or  $\text{F}^-$ , and template [3]. Hydrothermal methods comprise of aluminosilicate gel formation followed by aging and crystallization. The gel is formed by adding and mixing the structural element solutions in the presence of the mineralizer and template (if used) at designed temperature and time. During the synthesis process, the gel is kept at a fixed temperature in the range of 80–300 °C for specified aging and crystallization time at fixed pressure [3,7–9]. Examples of typical conditions for preparing different types of zeolites using hydrothermal (HT) methods are listed in Table 1 [7,8,10–15]. This method is widely used to prepare both micro- and nano-scale zeolites in laboratories and in the industry [7,9]. Advanced trends in zeolites synthesis aim to reduce the environmental impacts of the preparation process and engineer the properties of the produced materials; these trends include [10,12,15–27]:

- Producing green zeolites by using agricultural and industrial wastes as sources for the structural elements, e.g., fly and biomass ashes containing silicon, Aluminum ash and slag;
- Improving the performance of the solvo-thermal preparation method by using ionic liquid, where these liquids are used to improve the solvation power, reduce the vapor-pressure and increase the thermal stability of the produced zeolite;
- Producing green zeolites by reducing the consumption of chemicals and water; this trend is dependent on the use of alternative synthesis routes, e.g., vapor phase transition (Dry Gel Conversion), and mechano-chemistry processes;
- Preparation of hierarchical zeolite to enhance the accessibility of the pores; this trend relies on either the modification of the preparation scheme (bottom up) or post preparation modification (top down) techniques, Figure 2a,b illustrates these techniques;
- Preparation of zeolite nano-particles to improve the selective separation, to enhance the sorption and de-sorption properties, and subsequently to reduce the size of the wastewater processing units. The key factors that affect the properties of the prepared nano-zeolites are illustrated in Figure 2c;
- Preparation of nano-sheets (2D) to improve the performance of selective separation process by reducing the diffusion path and improving the catalytic activity.

These advanced trends in the preparation and modification of zeolites empowered the research and application of zeolites, especially in the field of water and wastewater treatment. In particular, the superior properties of nano-zeolites encouraged several researchers to explore the potential applications of nano-zeolites in this field. Different classes of nano-zeolites, i.e., nano-zeolite, and nano-zeolite composite, were prepared and tested for this purpose. The aim of this work is to summarize the current knowledge about the application of nano-zeolites in water and wastewater treatment, identify the gaps in this field, and highlight the challenges that face the wide-scale application of these materials. Within this context, the research and development in the application of nano-zeolite in sorption/ion exchange, photo-catalytic degradation, and membrane separation will be presented. To have insights into the scientific research interests in these applications,



analyses of the indexed research in Scopus database were conducted. This analysis was conducted for all the research indexed in that database without restricting the indexing time or language. The used keywords were selected to cover a specific application for zeolite and nano-zeolite, where the operators “AND” and “OR” were used to refine the search results and the annual research distribution over the last decade was visualized. For each application, the characterization, experimental testing, and theoretical analysis methodologies will be overviewed. The results of the most advanced research will be collected, summarized, and analyzed to allow an easy visualization and comparison of these research results. Finally, the gaps and challenges that face these applications will be identified.

**Table 1.** Examples zeolites hydrothermal preparation conditions (Reprinted with permission from [7]).

Exchanger	Preparation Conditions	Ref
Zeolite Na-A	Si:Al < 3, at 100 °C for 2–3 days	[8]
Zeolite Na-X	Si:Al ratios of 2.8:1, at 50 °C (6 h) * and 100 °C (3 h) for 2–3 days	[8]
Zeolite Na A-X blend	Si:Al ratios of 2:1, at 80 °C (2 h for gelification), 25 °C (24 h for ageing), and 90 °C (8 h for crystallization).	[10–12]
Clinoptilolite	Different silica, alumina and alkali molar ratios, temperatures (250–300 °C) and pressure (42.5–81.6 atm) for 2–5 days.	[13]
Analcite	Si:Al ratios of 2:1, at 275 °C for 2–3 days	[14]
Mordenite	Si:Al = 6:1 at 275 °C for 2–3 days	[14]
Zeolite y, nano scale	SiO <sub>2</sub> :Al <sub>2</sub> O <sub>3</sub> = 4.35:1, at 100 °C, 2 days	[15]

Note: \* induction period.

## 2. Advances in the Investigations of Nano-Zeolites as Ion-Exchanger/Sorbent

Zeolites are well known for their potential use in the removal of heavy metals, e.g., Zn, Hg, ... [17,28–30], organic contaminants, e.g., cationic surfactants, phenol [30,31], reducing excess ammonia [32,33], salinity, and acidity [34], and removal of radionuclides from aqueous radioactive waste effluents [10–12,15,35,36]. These applications are supported by their high cation exchange capacity and specific surface area. In addition, zeolites are characterized by high lattice stability, which entails the exchange of the charge compensating species without affecting the structure of zeolite. Moreover, the sorption processes that are designed to benefit from the molecular sieving, electrostatic fields, and polarizability are always reversible, which allow the reusability of this class of materials [5]. Nano-zeolites, inorganic- nano-zeolite composites, polymer-nano zeolite composites, and zeolites-nano-particle composites have been prepared and tested for contaminant removal either using sorption or ion/exchange batch techniques. The last category of materials, i.e., zeolites- nano-particle composite, relies on the modification of the micro-zeolite matrix using nano-particles; these applications are out of the scope of this work and could be found elsewhere [31]. An analysis of the research indexed in the Scopus database was conducted on the use of zeolites and nano-zeolite for “Removal” AND “Water” AND “Treatment” on 10 October 2021; the results are illustrated in Figure 3a–d. It is clear that the assessments of the potential use of zeolite and nano-zeolite in removal studies for water treatment represent nearly 47% of the research conducted in the field of removal studies (Figure 3a,c). The total amount of published research on the use of zeolite and removal is considerably high compared to that of nano-zeolite and removal. The annual numbers of indexed research have an increasing pattern from 2013 to 2020, with a noted reduction in 2021 (Figure 3b,d). Despite the ratio between the total indexed research for testing zeolite for removal and water treatment to that of nano-zeolite being nearly 1:0.045, this ratio

increased to 1:0.054–1: 0.076 during the period (2013–2021), where more than 82% of the indexed nano-zeolites research has been reported in that period. A recent review article reported that the indexed research about zeolite-based composites for adsorption of heavy metal in wastewater treatment in the Scopus database equals 180 research papers in the period (2011–2020) [31]. In another review article, the total indexed work in the Web of Science database during the period (1963–2018) on the use of zeolite with sodium/water/ion exchange/adsorption were reported to equal 311 references [34].

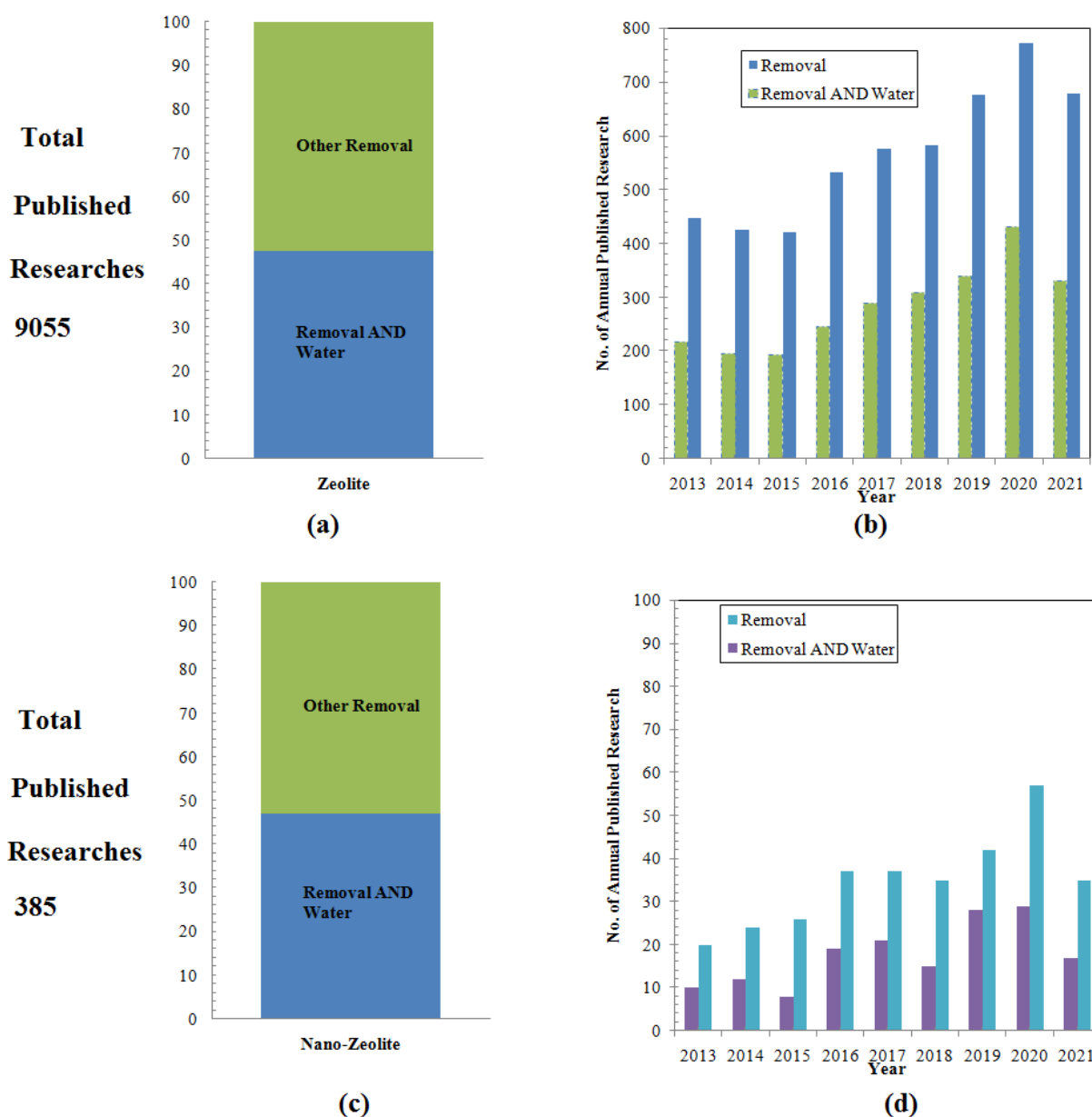


**Figure 3.** Analysis of the indexed work in the field of testing (a) Zeolite for “Removal” and “Removal AND Water Treatment”; (b) distribution of the total annual research for zeolites over the period (2013–2021); (c) Nano-zeolite for “Removal” and “Removal AND Water Treatment”; (d) distribution of the total annual research for Nano-zeolite over the period (2013–2021).

### 2.1. Testing Scheme to Optimize the Ion Exchange/Sorbent Applications

In general, the testing schemes for evaluating the performance of the ion-exchanger/sorbent materials include material characterization, operational conditions optimization, and design the removal process by adopting static batch and/or column operation. The aim

of the characterization step is to identify the chemical and physical properties of benefits to the ion-exchange/sorption processes. These include:

- Particle size, morphology, and surface properties determination: usually, these properties are determined using microscopic techniques. For nano-materials, Scanning Electron Microscope (SEM), Transmission Electron Microscope (TEM), and Scanning Probe Microscope (SPM) are widely used;
- Chemical compositions identification and detection of impurities: Spectroscopic analysis are widely used, e.g., Ultra-Violet Spectroscopy (UV), Fourier Transform Infra-Red Spectroscopy (FTIR), X-ray Photoelectron Spectroscopy (XPS), Energy-Dispersive X-ray spectroscopy (EDX);
- Material crystallinity: Wide Angle X-ray Diffraction (WAXD), Small Angle X-ray scattering (SAXS), and Ultra Small Angle Scattering (USAXS or USAXS) are widely used;
- Pore characteristics, the pore volume, porosity, and specific surface area could be measured via nitrogen absorption and application of Brunauer–Emmett–Teller (BET) model;
- The tendency of the material to agglomerate is usually identified by measuring zeta potential and the hydrodynamic radius;
- The ability of the material to act as cationic or anionic exchanger is usually determined by identifying the zero point charge;
- Cation Exchange Capacity (CEC) procedures are widely used to assess the capacity of the cationic exchanger.

The features of the above-mentioned characterization techniques are listed elsewhere [37]. In addition, chemical and thermal stabilities of the materials are important to be identified for materials used under challenging operational conditions, i.e., treating alkali or acidic media, and at high ambient temperature.

The optimization of the operating conditions could be conducted by relying on One Factor at A Time (OFAT) technique or the Multi Variant Technique (MVT) to identify the optimum ion-exchanger/sorbent mass ( $m$ , g), contaminated solution volume ( $V$ , L) and pH, initial contaminant concentration ( $C_o$ , mmol/L), mixing velocity ( $v$ , rpm), contact time ( $t_{eq}$ , min), and operational temperature ( $T$ , K). Table 2 summarizes the features of each technique [38,39].

**Table 2.** Comparison between the optimization techniques (Reprinted with permission from [39]).

Technique	Feature	Advantage	Limitation
OFAT	Evaluate isolated effects of the studied factors on a single performance measure Empirical, mechanistic, and black box models are used to analyze the data	Allow the determination of mechanisms, interpolate and extrapolate the process performance	Does not allow the determination of the effect of interaction between the factors that affect the performance
MVT	Evaluate the effects of the studied factors variability and their interactions on single and multi performance measures	Identify the main influencing factors, Provide insights into the system reliability	Does not allow the determination of the mechanism

## 2.2. Batch Investigations

Batch investigations of ion-exchanger/sorbents materials are used to support the design of the removal process. In this regard, kinetic and equilibrium studies are conducted to allow the calculations of the rate constants, material capacity, and the thermodynamic parameters. In these investigations, certain mass of the ion-exchanger/sorbent ( $m$ , g) is mixed with certain volume of the contaminated solution ( $V$ , L) of specified contaminant concentration ( $C_o$ , mmol/L) and pH at specified mixing speed for a certain period of time at determined temperature ( $T$ , K). Then, the solid/liquid suspension is separated and the contaminant concentration ( $C_t$ , mmol/L) in the solution is measured using suitable



analytical techniques. The sorbed contaminant amount ( $q_t$ , mmol/g) is determined using the following equation:

$$q_t = \frac{(C_o - C_t)V}{m} \quad (3)$$

Kinetic batch investigations are used to determine the time to reach equilibrium and predict the rate constants and maximum sorbed contaminant amount. Both rate and mechanistic models are used to analyze the kinetic behavior of the removal process obtained using an OFAT technique, where Pseudo-First Order (PFO), Pseudo-Second Order (PSO), Double Kinetic Model (DKM), and Elovich (El) rate models are widely used to determine the rate constants. Intra-particle model (IPM) and homogenous particle diffusion model (HPM) are used to determine the rate determining mechanism and calculate its parameters. The equilibrium behavior is investigated by varying the initial contaminant concentration within a specified range following the OFAT technique, and then the data are analyzed using a suitable model, i.e., Freundlich (F), Langmuir (L), and D-R models. Table 3 lists the features of these widely used models. Running the experiments at different temperatures is an important step to optimize the operating temperature and to determine the thermodynamic parameters of the reaction (Table 3). These parameters could be determined either from the kinetic data at equilibrium values, where each curve represents a single point in the equilibrium, or determined from the equilibrium behavior data.

**Table 3.** Models used in analyzing the results of batch investigations for ion-exchanger/sorbents.

Model	Equation	Model Features
KINETIC	PFO Linear : $\log(q_e - q_t) = \log(q_e) - \frac{k_1}{2.303} t$ Non – linear : $q_t = q_e (1 - e^{-k_1 t})$	Rate model used to determine the rate constant ( $k_1$ , min <sup>−1</sup> ) and sorbed contaminant amount per unit mass of zeolite at equilibrium ( $q_e$ , mmol.g <sup>−1</sup> ), Entails that the reaction rate is limited by only one process or mechanism on a single class of sorbing sites and that all sites are of the time dependent type, The reaction might be controlled by diffusion through the boundary layer.
	PSO Linear : $\frac{t}{q_t} = \frac{1}{k_2 q_e^2} + \frac{1}{q_e} t$ Non – linear : $q_t = \frac{k_2 q_e^2 t}{1 + k_2 q_e t}$	Rate model used to determine the rate constant ( $k_2$ , g.mmol <sup>−1</sup> .min <sup>−1</sup> ) and sorbed contaminant amount per unit mass of Zeolite at equilibrium ( $q_e$ , mmol.g <sup>−1</sup> ), Entails that the rate of sorption is directly proportional to the number of active surface sites and that the rate limiting step may be a chemical sorption involving valence forces through sharing or exchange of electrons between the adsorbent and the adsorbate.
	DKM $q_t = q_e - \left( \frac{D_1}{M} e^{-k_{d1} t} \right) - \left( \frac{D_2}{M} e^{-k_{d2} t} \right)$	A rate model that assumes that the reaction proceed via two subsequent mechanisms. It allows the calculation of the sorbed amount of contaminant in at equilibrium and identification of the rate constant for each mechanism
	EL Linear : $q_t = \beta \ln(\beta \alpha) + \beta \ln(t)$	Used to determine the initial sorption rate ( $\alpha$ , mEq.g <sup>−1</sup> .min <sup>−1</sup> ) and the desorption constant ( $\beta$ , mmol.g <sup>−1</sup> ). Entails that the reaction increases exponentially with time.
	IPM $q_t = K_{pi} \sqrt{t} + C_{pi}$	Used to quantify the boundary layer effect ( $C_{pi}$ , mmol.g <sup>−1</sup> ), and determine the rate constant of the sorption stage ( $K_{pi}$ , mmol.g <sup>−1</sup> .min <sup>−0.5</sup> ), Entails that the reaction involves diffusion mechanism and allow the assessment of the contribution of the boundary layer in the reaction
	HPM Film : $-\ln(1 - X) = \frac{3DC}{r\delta q} t$ Particle : $-\ln(1 - X^2) = \frac{3D_i \pi^2}{r^2} t$	Used to determine the rate controlling step and calculate the diffusion coefficient ( $D$ , m <sup>2</sup> /s), Film diffusion model entails that the rate determining step is the contaminants diffusion through the liquid film around the Zeolite particles, Particle diffusion model entails that the rate determining step is the contaminants diffusion into the Zeolite particles.

Table 3. Cont.

Model	Equation	Model Features
ISOTHERM	Linear : $\log q_e = \log K_f + (1/n) \log C_e$	Used to determine Freundlich constant indicative of the relative adsorption capacity ( $K_f$ , mmol.g <sup>-1</sup> ), Freundlich intensity constant indicative of the relative sorption capacity ( $n$ ),
	Non – linear $q_e = K_f C_e^{\frac{1}{n}}$	Empirical model employed to describe the interaction between contaminants and heterogeneous sorbent, It suggests that sorption energy exponentially decreases on filling of the sorption centers of the sorbent.
	Linear : $\frac{C_e}{q_e} = \frac{1}{Q^\circ b} + \frac{1}{Q^\circ} C_e$	Used to determine the mono-layer capacity ( $Q^\circ$ , mmol.g <sup>-1</sup> ) and Langmuir constant ( $b$ )
	Non – linear : $q_e = \frac{Q^\circ b C_e}{1 + b C_e}$	Assumes that the sorption takes place at specific homogenous sites, energetically equivalent, within the sorbent, The sorbent has a finite capacity for the contaminants.
	Linear : $\ln(q_e) = \ln(q_m) - \beta \varepsilon^2$ $\varepsilon = RT \ln\left(1 + \frac{1}{C_e}\right), E = \frac{1}{\sqrt{-2\beta}}$	Used to determine the maximum amount of ion that can be sorbed onto unit weight of zeolite ( $q_m$ , mmol.g <sup>-1</sup> ) constant related to sorption energy (mol <sup>2</sup> .K.J <sup>-2</sup> ), Polanyi sorption potential, $\varepsilon$ is the work required to remove a molecule to infinity from its location in the sorption space,
	Non – linear : $q_e = q_m \exp\left(\frac{-\varepsilon^2}{-2E^2}\right)$	Employed to describe the interaction between contaminants and heterogeneous sorbent, Used to differentiate between physical and chemical sorption.
Thermo	$\Delta G^\circ = -RT \ln(k_c)$ & $\Delta G^\circ = \Delta H^\circ - T\Delta S^\circ$	Used to determining the thermodynamic parameters, i.e., Gibbs free energy change ( $\Delta G$ , KJ.mol <sup>-1</sup> ) and the change in entropy ( $\Delta S$ , kJ.mol <sup>-1</sup> .K <sup>-1</sup> ) and in enthalpy $\Delta H$ , kJ.mol <sup>-1</sup> ) from the real thermodynamic equilibrium constant ( $K_c$ ).

The reusability and regeneration ability of the ion-exchanger/sorbent is an important topic to be identified to ensure the economic feasibility of the materials and to reduce the environmental footprint by reducing the material requirement for the treatment process. The reusability is usually tested by repeated loading of the ion-exchanger/sorbent with the contaminant; this is only useful if the material did not reach each its capacity. The regenerability is the use of eluent to de-sorb the contaminant from the ion-exchanger/sorbent, and re-load the material with the contaminant in successive cycles. The latter set of investigations includes optimization of the eluent (e.g., HCl, HNO<sub>3</sub>, NaOH), elution time, eluent volume to ion-exchanger/sorbent mass ratio, and regeneration cycles [7,38]. It should be noted that the repeated use of the ion-exchanger/sorbent in reusability and regeneration ability is associated with a decrease in the removal efficiency, as the active sites become occupied or not fully recovered, respectively.

### 2.3. Application in Removing Radioactive Contaminants

Zeolites have been used for several decades as an ion-exchanger on the industrial scale in the nuclear industry. In particular, natural CLP is being used in a Site Ion-EXchange effluent Plant SIEXP, City, UK [40]. Several studies were dedicated to assess the potential use of natural and synthetic zeolites as potential materials for radio-contaminants [40–67] and metal ion removals [67–84]. The tested zeolites included natural zeolites, modified natural zeolites, nano-zeolites, and nano-zeolite-composites in the form of magnetic or polymeric materials. In this sub-section, the focus is to present the research related to radioactive contaminants removal, where, in the next sub-section, the metal ions (Section 2.4.1) and organic contaminant (Section 2.4.2) removal will be discussed. Scopus database search retrieved 17 research papers (eight of them target the immobilization step) of the search (Nano AND zeolite AND radioactive AND Cs Or Sr OR Th Or U Or Eu). Table 4 summarizes the tested nano-zeolite type, size, if it is a composite and the preparation method. Moreover, the results of the kinetic, equilibrium, thermodynamics, and regeneration ability investigations of this research are listed. Based on the presented data, it could be concluded that:

- Different types of synthetic nano-zeolite were investigated that include zeolite A, zeolite Y, zeolite X, CHA, and MOR. The listed research employed the hydrothermal (HT) preparation method and mostly utilized analytical grade chemicals during the preparation.

- Both magnetic and polymeric Nano-zeolites composites were tested for the removal of the radioactive contaminants. In particular, natural zeolite was ground to nano-scale then immobilized in polymeric matrix, i.e., Poly vinyl alcohol(PVA), Alginate (ALG)/poly-ethyleneoxide (PEO), and tested.
- All of the listed research was conducted by using single contaminant solution, where inactive contaminants were used to reduce the radiological exposure of the researchers.
- The investigated sorbent mass to waste volume fall in the range ( $1 \leq m/V \leq 20$ ), where regeneration studies are limited to one study.

The examination of the listed data indicates that radioactive contaminants removal reactions are mostly best described using the PSO rate model, which indicates the chemisorption nature of the reaction that involves electron sharing between the contaminants and the zeolite [11,15,28,31,35,38,41–87]. For all the reported reactions, the kinetic data can be divided into two portions; the first is fast with a steep slope that is linked to the sorption onto the boundary layer and the second is slower approaching an asymptote which is closely related to particle diffusion [28,40,41,43,44,61–91]. The Langmuir isotherm model is the best model to describe the equilibrium behavior where monolayer capacity is used as a comparative parameter to measure the affinity of the sorbent to a specific contaminant. Except for Lee et al. [64], the removal reactions are spontaneous and an endothermic process with increased sorbent disorder ( $-ve \Delta G$ ,  $+ve \Delta H$ , and  $+ve \Delta S$ , respectively). The values of  $\Delta H$  in the range ( $2 < \Delta H < 40$  kJ/mol) that refer to hydrogen bonding between the radio-contaminant and the sorbent. It should be noted that the thermodynamic parameters calculated by Lee et al. were determined at a single initial concentration experiment (100 ppm) at three temperatures, which is a represent for the reaction at this particular contamination level not the system at varying initial concentrations [64]. Only three research studies adopted both OFAT and MVT to study and optimize the removal process [15,65,66]. The above-mentioned discussions and presented research indicate clearly that limited research efforts have been made to study the application of nano-zeolite in removing anionic uranium species and iodide [85–87], removal from binary or more complicated solutions [38,64,65,88,92], and the impregnation of nano-zeolite [93,94]. Usually, the removal mechanism is based on the radio-contaminant interaction with active OH sites in the nano-zeolite, where the radio-contaminant is exchanged with  $H^+$  or  $Na^+$ . For Nano-zeolite composites, the removal process will occur on the active sites in zeolite and the polymer or the magnetic components. An illustrative example for the mechanism is presented in Figure 4, for Th(IV) and U(VI) ions sorbed onto Poly vinyl alcohol(PVA)/Sodium Alginate (SA)/poly-ethyleneoxide (PEO)/HZSM5 nano fiber adsorbent, where the radio-contaminants interact with the negatively charged nano fiber adsorbent or via electron exchange from adsorbent surface to Th(IV) and U(VI) ions. It was reported that OH and COOH groups in that sorbent could be dissociated into O and COO groups in water systems and contribute to the sorption process [65].

**Table 4.** Batch investigations of nano-zeolites applications in radioactive contaminant removal.

Cont.	Nano-Zeolite				m/Vg/L	Kinetic Investigations					Capacity	Thermodynamic Parameters			Regeneration	Ref.
	Type	Size, nm	Composite	Preparation		$C_o$ , mmol/L	pH	$t_{eq}$ , min	Temp, K	Model		$Q^o$ @RT mmol/g	$\Delta H$ kJ.mol <sup>-1</sup>	$\Delta S$ J.mol <sup>-1</sup> .K		
Cs <sup>1</sup>	Zeolite Y	20–50	-	HT, Chemicals	2	5.82	6	60	298–313	PSO	6.72	-	-	-	-	[15] MVT
	Zeolite Y	<100	Mangetite		2	-	-	-	-	-	1.17	2.75	35	7.93	-	[61]
	Zeolite A	>50	Magnetic		10	10	8	120	298	PSO	1.724	3.08	60	15.0	-	[62]
	CHA	<510	-		1	0.752	-	1	RT	PSO	0.3	-20.02	−14	15.8	-	[64]
	Zeolite A	82 ± 9	-	HT, fly ash	10	0.752	7	1440	RT	-	-	-	-	-	-	* [67]
	Zeolite X	86 ± 12	-	HT, fly ash	10	0.752	7	1440	RT	-	-	-	-	-	-	-
Eu <sup>3</sup>	MOR1	Sphere, D = 50	-	HT, Chemicals	4	3	1	1440	303 ± 1	PSO	2.72	8.81	74.75	13.8	-	[63]
	MOR2		-								2.87	7.05	69.75	14.1	-	
	MOR3	Rod, L = 400, D = 25:50	-								2.98	9.64	79.02	14.3	-	
	MOR4		-								3.50	10.15	82.84	14.9	-	
Sr <sup>2</sup>	Zeolite Y	20–50	-	HT, Chemicals	2	19.72	6	60	298–313	PSO	15.42	-	-	-	-	[15] MVT
	Zeolite Y	<100	Mangetite		2	-	-	-	-	-	1.38	8.43	41	7.16	-	[61]
	Zeolite A	>50	Magnetic		10	20	8	120	298	PSO	1.016	12.16	100	18.1	-	[62]
	CHA-3	100–300	-	HT, Chemicals	10	1.14	-	60	298	PSO	0.131	-	-	-	5	[54]
	Zeolite A	82 ± 9	-	HT, fly ash	10	1.14	7	1440	RT	-	-	-	-	-	-	* [67]
	Zeolite X	86 ± 12	-	HT, fly ash	10	11.4	7	1440	RT	-	-	-	-	-	-	* [67]
Th <sup>4</sup>	Natural	109.9	PVA/ALG	-	20	0.285	6	120	298	PSO	-	-	-	-	-	[76]
	MOR1	Sphere, D = 50	-	HT, Chemicals	4	4	1	1440	303 ± 1	PSO	1.18	11.74	75.86	11.2	-	[63]
	MOR2		-								1.23	11.2	73.65	11.3	-	
	MOR3	Rod, L = 400 D = 25:50	-								1.11	11.78	78.72	11.0	-	
	MOR4		-								1.55	9.74	71.20	11.8	-	
	U <sup>4</sup>	HZSM-5	Fiber D = 98	PVA/ALG/PEO	HT, Chemicals	1	-	5.5	240	298	DKM	1.138	35.67	145.3	7.704	-
ZSM5		-	PVA/ALG/PEO	HT, Chemicals	1	0.517	5	150	298	DKM	0.569	25.962	97.2	3.039	-	[66] MVT
U <sup>4</sup>	HZSM-5	Fiber D = 98	PVA/ALG/PEO	HT, Chemicals	1	-	5.5	240	298	DKM	0.577	21.34	81.9	3.11	-	[65] MVT

Note: \* Crystallite size.

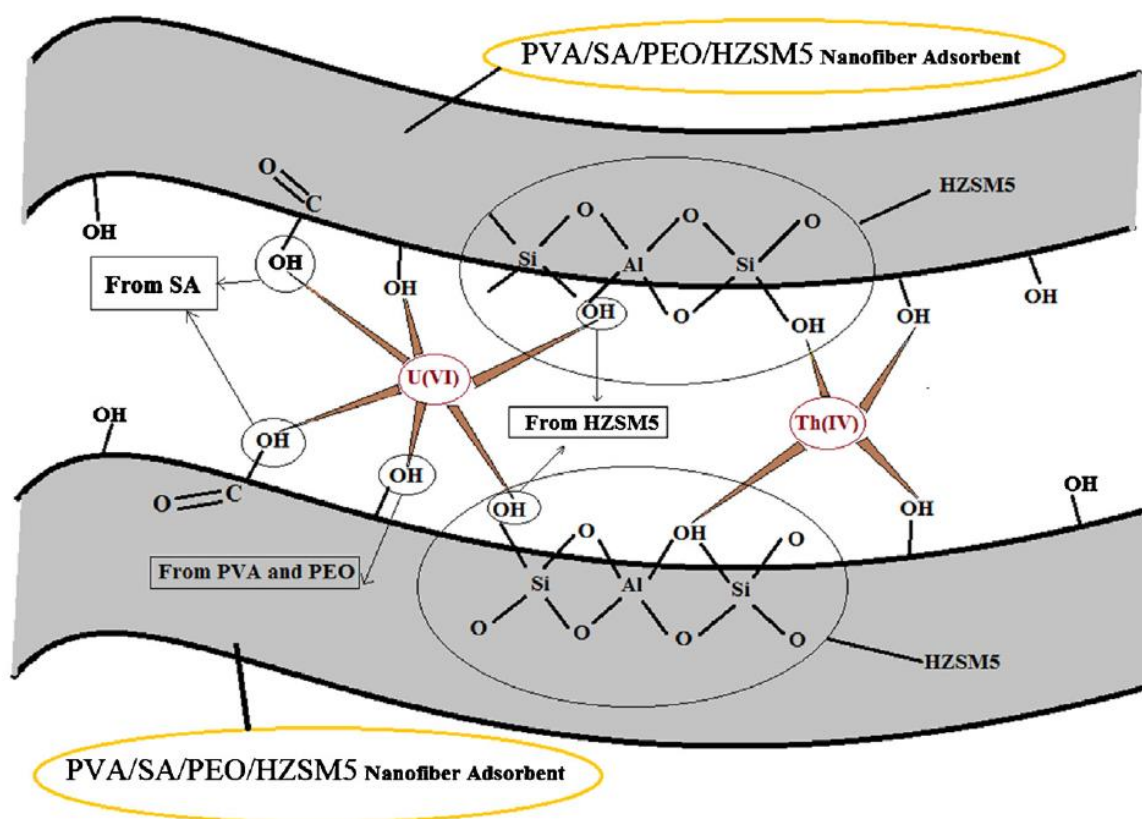


**Figure 4.** The sorption mechanism of Th(IV) and U(VI) ions on to the PVA/SA/PEO/HZSM5 nanofiber adsorbent (Reprinted with permission from [65]).

#### 2.4. Application in Industrial Wastewater Treatment

Zeolites have been tested for their applications as ion-exchangers in industrial wastewater treatment, where most of the applications focused on using zeolites as a cationic exchanger. Fewer investigations were devoted to examining the potential use of zeolite as an anionic exchanger, where the zeolites surface should have a permanent positive charge to ensure its performance. This is achieved via operating the removal process under the zero point charge or modifying the surface of zeolite [95–117]. In this case, the design of the process should consider the nature of the zeolites as amphoteric materials that tend to buffer the acidic and alkaline solution pH to 3.5–8 to equilibrate to the zero point charge and have a noted solubility in acidic media [38,96,118,119]. In this subsection, the application of nano-zeolites in metal removal and organic contaminant sorption will be summarized.

##### 2.4.1. Metal Removal Studies

The search in the Scopus database using the keywords (Nano AND zeolite AND metal AND sorption) returned 53 research works. These results cover the removal of radio-contaminants and carbon dioxide, modification of zeolites for its application as catalyst, and ion-exchange/sorption applications, including application of zeolites-nanocomposites. Table 5 lists the investigations that addressed the use of nano-zeolite in metal removal [68–71,73–76,78–84]. The following remarks could be drawn from the table:

- All the listed studies investigated only magnetic and polymeric composites, not the nano-zeolite particles. The magnetic composites included the use of magnetite and cobalt ferrite, where polymeric composites include various single and binary polymer, e.g., PVA, chitosan, ...
- Different types of natural and synthetic nano-zeolites were investigated. Natural zeolites were not identified or presented as CLP, where the synthetic nano-zeolites include zeolite Na-X, zeolite Y, Faujasite (FAU), ZSM-5, HZSM5, and MOR. The listed



research employed the hydrothermal (HT) preparation method and one research work investigated the use of silica and alumina wastes for the preparation of the nano-zeolite.

- All of the listed research was conducted by using a single contaminant solution, the sorbent mass to volume ratio fall in the range ( $0.5 \leq m/V \leq 20$ ) and regeneration studies were investigated in a comparatively large amount of research.

By examining the presented research results in Table 5, it is clear that the reactions follow PSO and Langmuir models. The removal reactions are spontaneous with increased sorbent disorder ( $-ve \Delta G$ , and  $+ve \Delta S$ , respectively). All the reactions are endothermic except the metal ion reactions with the FAU/Geopolymer matrix and MOR/PEG-EG. They are exothermic with a respective high change in enthalpy that falls in the range of a chemical reaction ( $\Delta H > 60 \text{ kJ/mol}$ ). Only two research works utilized the OFAT and MVT to study and optimize the removal process [82,84]. In research that compared the nano-zeolite with their polymeric composites, the analysis of the mechanism of metal ion removal in nano-zeolite- polymeric composites refers to the role of the polymeric composites in enhancing the removal by providing more active sites for the reactions. In case of Mn removal by CLP/Glutamic acid, the complexation with the organic active groups and zeolite sites were reported to be responsible for the sorption [82]. As the availability of the negative charges on the surface of the ion-exchanger/sorbent is essential for the successful application of the material in the cation removal, it should be noted that the presence of the magnetite/polymer affects the behavior of the sorbent at different pH [38,76,90]. At low pH, the surface of nano-zeolite/polymer has a positive charge that hinders cation removal from the solution. As the pH increases, the COOH groups deprotonate, allowing for the presence of a negative charge on the surface of the sorbent. A schematic representation of the pH effect on the availability of the negative charge on nano-zeolite/PVA/ALG is illustrated in Figure 5. As the pH increases, the hydroxyl species of the metals will become dominant and will precipitate [76,90].

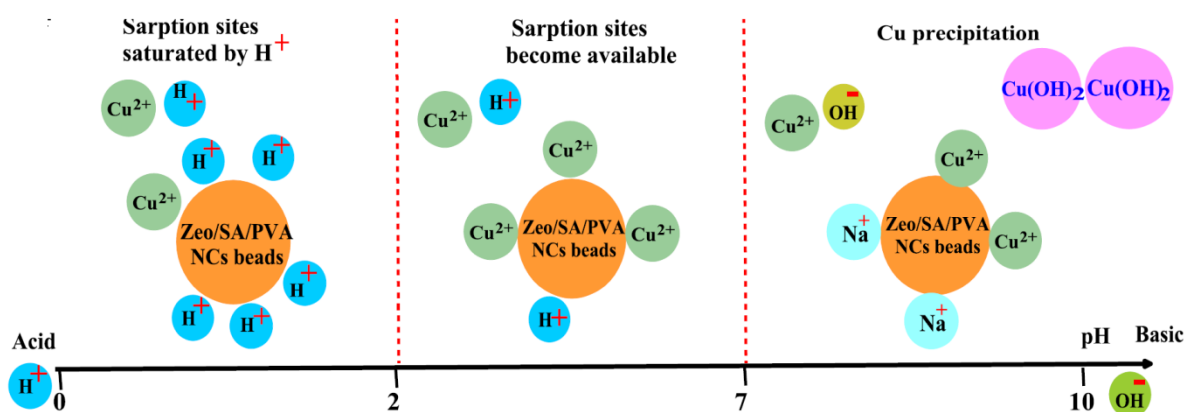


**Figure 5.** Effect of pH on the adsorption of heavy metals (ex.:  $\text{Cu}^{2+}$ ) onto nano-Zeolite polymeric (Reprint with permission from [76]).

**Table 5.** Investigations of nano-zeolite in cation removal form single contaminant solutions.

Cont.	Nano-Zeolite				m/Vg/L	Kinetic Investigations				Model	Capacity	Thermodynamic Parameters			Regeneration	Ref.
	Type	Size, nm	Composite	Preparation		$C_0$ , mmol/L	pH	$t_{eq}$ , min	Temp, K		$Q^0$ @RT mmol/g	$\Delta H$ KJ.mol <sup>-1</sup>	$\Delta S$ J.mol <sup>-1</sup> K	(-) $\Delta G$ @RT KJ.Mol <sup>-1</sup>		
Al <sup>3</sup>	Natural	109.9	PVA/ALG	-	20	0.926	6	120	298	PSO	0.438	-	-	-	10	[76]
As <sup>3</sup>	-	50	Magnetite	-	16	1.33	-	60	-	-	0.059	-	-	-	-	[73]
Cd <sup>2</sup>	Zeolite NaX	Fiber >170	PVA	HT, chemicals	0.5	0.446	5		298–318	PSO	7.279	11.099	82	13.24	5	[75]
	-	109.9	PVA/ALG	Natural	20	0.222	6	120	298	PSO	0.411	-	-	-	10	[76]
	CLP	-	DTPA	Natural	0.2	8.763	5.9	205	-	PSO	1.235	−10.3	102.89	−20.4	-	[84] MVT
Co <sup>2</sup>	FAU	<150	Geopolymer	HT, Si & Al wastes	2	4.237	8	20	298	PSO	2.27	−106.88	323	203.1	-	[70]
	ZSM-5	-	PVA/ALG	HT, chemicals	1	1.695	-	240	298	DKM	1.255	16.47	55	0.16	-	[69]
	-	12	GLU	Natural	10	10	-	360	298	PSO	0.179	-	-	-	-	** [79]
	CLP	59	APS	Natural	5	9.448	-	300	298	PSO	1.36	-	-	-	-	** [80]
Cu <sup>2</sup>	FAU	<150	Geopolymer	HT, Si & Al wastes	2	3.937	8	20	298	PSO	1.987	−150.76	464	239	-	[70]
	-	109.9	PVA/ALG	Natural	20	0.394	6	120	298	PSO	0.764	-	-	-	10	[76]
	CLP	<40	CYS	Natural	15	7.874	-	1800	298	PSO	0.521	-	-	-	-	** [81]
Fe <sup>3</sup>	-	109.9	PVA/ALG	Natural	20	0.448	6	120	298	PSO	0.845	-	-	-	10	[76]
Li <sup>3</sup>	-	109.9	PVA/ALG	Natural	20	3.62	6	120	298	PSO	5.527	-	-	-	10	[76]
Mn <sup>2</sup>	Natural	109.9	PVA/ALG	Natural	20	0.455	6	120	298	PSO	0.781	-	-	-	10	[76]
	CLP	-	GLU	Natural	5	10.6	3.5	120	298	PSO	0.101	-	-	-	4	** [82] MVT
Ni <sup>2</sup>	Zeolite NaX	Fiber >170	PVA	HT, chemicals	0.5	0.341	5		298–318	PSO	5.738	6.018	60	11.9	-	[75]
	-	109.9	PVA/ALG	Natural	20	0.426	6	120	298	PSO	0.812	-	-	-	10	[76]
	CLP	-	DMG	Natural	10	1.707	5.5	1400	298	PSO	0.96@293	-	-	-	-	** [83]
Pb <sup>2</sup>	FAU	150–250	Cobalt ferrite	HT, Chemicals	-	1.038	7	60	298	PSO	2.91	-	-	-	-	[68]
	Zeolite Y	150–300	-	HT, Chemicals	0.4	0.483	6	60	299	PSO	2.19	-	-	-	-	[71]
		30–50	chitosan								0.265	-	-	-	-	[71]
	-	109.9	PVA/ALG	Natural	20	0.121	6	120	298	PSO	0.229	-	-	-	10	[76]
	HZSM-5	Fiber	PVP/chitosan	HT, chemicals	1	0.48	5.5	240	298	DKM	1.46	78.35	146.68	8.22	-	[74]
	MOR	35.50,	PEG-EG	HT, chemicals	3	0.241	8	180	298	PSO	0.084	−68.82	218	133.7	5	[78]
Zn <sup>2</sup>	FAU	<150	Geopolymer	HT, Si & Al wastes	2	3.823	8	20	298	PSO	2.017	−83.1	250	154.0	-	[70]
	-	109.9	PVA/ALG	Natural	20	0.382	6	120	298	PSO	0.739	-	-	-	10	[76]

Note: \*\* thermodynamics are determined from kinetics. EG = ethylene glycol. PEG = polyethylene glycol 200. GLU = glutamic acid. DMG = dimethylglyoxime. DTPA = diethylenetriaminepentaacetic acid.

#### 2.4.2. Organic Contaminants' Sorption Studies

The bibliometric data in Scopus include 77 research works on the (Nano AND zeolite AND organic AND removal); these research works include the use of modified nano-zeolite, nano-zeolite, and zeolite-nano-composite in membrane separation, catalysis, and dual processes. Most of the relevant papers addressed the use of nano-zeolite in dye, BisPhenolS (BPS), and Polycyclic Aromatic Hydrocarbons (PAH) removal using the ion-exchange/sorption technique only, as indicated in Table 6 [72,77,120–128]. Table 6 displays the data related to dye removal; the following remarks could be summarized from these researchers:

- Natural and synthesized nano-zeolites of different types, i.e., Nano-zeolites X, MOR, ZSM5, and Sodalite were investigated, where both green and conventional preparation routes were adopted,
- Nano-zeolite particles were mainly investigated for the removal of different types of dyes, i.e., MG, CV, MB, BR (18,41,46), and only one research studied the polymeric composite of natural nano-zeolite. No study addressed the inorganic nano-zeolite composite,
- The sorbent dosage falls in the range (0.3–10), which is relatively narrower than those studied for the radioactive contaminants and for metal removal studies.
- The studies were conducted using single contaminant solution and the regenerability studies are very limited.

By examining the kinetic data in Table 6, the removal reactions are chemisorptions, i.e., follow PSO, where Langmuir and Freundlich were found to be the best models to describe the equilibrium behavior. The available data indicate that the reactions are mostly spontaneous and endothermic. The values of  $\Delta H$  in the range ( $2 < \Delta H < 40$  kJ/mol) that refer to hydrogen bonding between the organic contaminants and the sorbent. In addition to the listed data, ZSM-5 nano-zeolite (250 nm) was prepared via hydrothermal methods using chemicals, and was modified using hexadecyltrimethylammonium bromide (HDTMA-B); the reaction follows PSO and reaches equilibrium at 120, min ( $C_0 = 5$  mg/L, pH = 4, RT), and the reaction follows Freundlich with Langmuir monolayer capacity = 41 mg/g [123]. This work revealed that, for single layer HDTMA-B formation on the external surface of the nano-zeolites, BPS sorption is very low due to the unavailability of sufficient positive sites onto the sorbent. Finally, the surface of ground natural zeolite (170 nm) was modified using humic acids, and it was found that this Hybrid sorbent allowed anthracene and pyrene removal at percentages higher than 90%; fluoranthene, of angular molecular structure, was adsorbed at 85% [128].

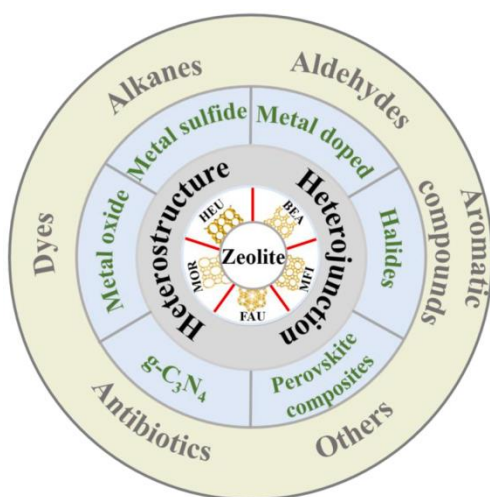
**Table 6.** Applications of Nano-zeolites in dye sorption.

Cont.	Nano-Zeolite			Preparation Technique	m/Vg/L	Kinetic Investigations				Capacity	Thermodynamic Parameters			Regeneration	Ref.	
	Type	Size, nm	Composite			$C_o$ , mg/L	pH	$t_{eq}$ , min	Temp, K	Model	$Q^o$ @RT mg/g	$\Delta H$ kJ.mol <sup>-1</sup>	$\Delta S$ J.mol <sup>-1</sup> K			(-)ΔG @RT kJ.mol <sup>-1</sup>
AB-74	Zeolite	40–500	PA-6	Natural		20	-	120	-	PSO	166.66	-	-	-	-	[72] MVT
MG	ZF	46.56	-	HT, Al waste and Si chemical	2	700	-	120	RT	PSO	226.757	−5.819	19	11.48	-	[77]
	ZM	26.28	-		2	700	-	180	RT	PSO	239.234	−5.715	14	9.887	-	[77]
	ZS	75.83	-		2	50	-	40	RT	PSO	29.744	−22.62	65	41.99	-	[77]
	ZT	38.73	-		2	50	-	50	RT	PSO	25.221	−22.473	69	43.03	-	[77]
CV	Sodalite	40–90	-	Low- temp, chemicals	0.3	20	-	40	RT	PSO	227.2	28.006	108.22	4.225		* [120]
	Zeolite X	19–39	-	HT, coal fly ash	0.75	-	-	-	-	PSO	234.57	-	-	-	10	[126] MVT
MB	Zeolite-X	170	-	HT, Chemicals	2.5	100	-	5	RT	PSO	0.1	-	-	-	-	[121]
	MOR	55.34	-		10	-	-	120	RT	PFO	1.72	−18.98	4.6	17.6	-	[122]
BR-41	ZSM5	40–100	1.2		17, M		60	RT	PSO	13.76, μM/g	-	-	-	-		
BR-18			1.2		33, M	7	60	RT	PSO	28.49, μM/g	-	-	-	-	[125] MVT	
BR-46			1.2		20, M		60	RT	PSO	27.6, μM/g	-	-	-	-		

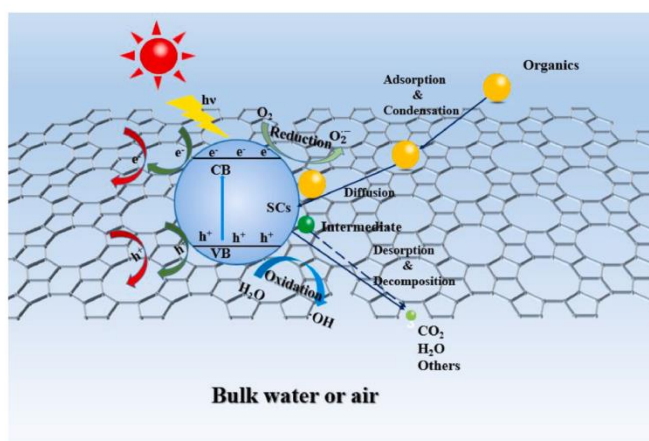
Note: \* Crystallite size. AB = Acid Blue. MG = Malachite Green. CV = Crystal Violet. MB = Methylene Blue. BR = Basic Red. ZF = fumed silica- based zeolite. ZM = sodium metasilicate-based Zeolite. ZS = silica gel- based zeolite. ZT = tetraethyl orthosilicate-based zeolite.

### 3. Advances in Nano-Zeolite-Composites Applications in Photo-Catalytic Degradations

Advanced oxidation processes (AOP) are widely applied as tertiary wastewater treatment technologies that aim to convert persistence contaminants into simple biodegradable and harmless products [2,129]. These technologies rely on the use of single or combined activation method to generate reactive species that can degrade these contaminants. Different activation methods are available including photochemical, chemical, and ionizing radiation [2,130]. Photo-catalytic degradation is one of these technologies that utilizes photon excitation of the catalyst to generate electron ( $e^-$ ) and hole ( $h^+$ ) pairs, i.e., primary radicals, that subsequently hydrolyzes the water molecules to form different types of secondary radicals that will react with the contaminants. Meanwhile, part of the primary radicals recombines with the catalysts surface which reduces the photo-catalytic activity. A large variety of metal oxides, zero-valance elements, and bi-metallic materials were investigated and applied as a catalyst to generate primary radicals, i.e.,  $TiO_2$ ,  $ZnO$ ,  $Fe^0$ ,  $Cu^0$ , and  $Zn/Pd$  [37,129,131]. To engineer sunlight driven photo-catalytic degradation process, there is a need to select the catalyst to have a narrow band gap sufficient to capture the solar energy, adequate sorption sites and reaction centers, efficient separation and transfer of the primary radicals, minimum photochemical corrosion, allow easy separation, and have low agglomeration tendency [129,132]. Modifying the catalyst and the use of support were proposed in this context. The support should possess high specific surface area, acceptable hydrophobicity especially for organic contaminant degradation and excellent stability in water. CLP, ZSM-5, zeolite-Y, MOR, and zeolite beta were tested for their applications as support not only due to their excellent sorption properties but also due to the presence of acid/base sites that can reduce the  $e^-$ - $h^+$  recombination. Figure 6a summarizes the application of zeolite-composite in the degradation of different organic contaminants in wastewater and in air. The photo-catalytic degradation mechanism of these composites is illustrated in Figure 6b; the mechanism comprises the adsorption and diffusion of the contaminants on the zeolite surface, photo-catalytic degradation, and decomposition/desorption. Different techniques are available to prepare these composites including ex-situ, sol-gel, ionic exchange, hydrothermal synthesis, and impregnation techniques. A detailed review of the preparation techniques is presented elsewhere [129].



(a)



(b)

**Figure 6.** (a) Applications of zeolite-composite in the degradation of different organic contaminants in wastewater and air; (b) schematic of adsorption and photo-catalytic degradation on the surface of zeolite-based composites (Reprinted with permission from [129]).



The analysis of the bibliometric data in the Scopus database indicated that there are 450 research works that addressed the (zeolite AND photodegradation) and 68 research works addressed the (nano AND zeolite AND photodegradation). By restricting the search using the word “Water”, the number reduces to 151 and 21, respectively. The annual distribution of these researches are illustrated in Figure 7a,b; the figure illustrates the increasing research trends for the application of zeolites and nano-zeolite in the photo-degradation of contaminants in water.

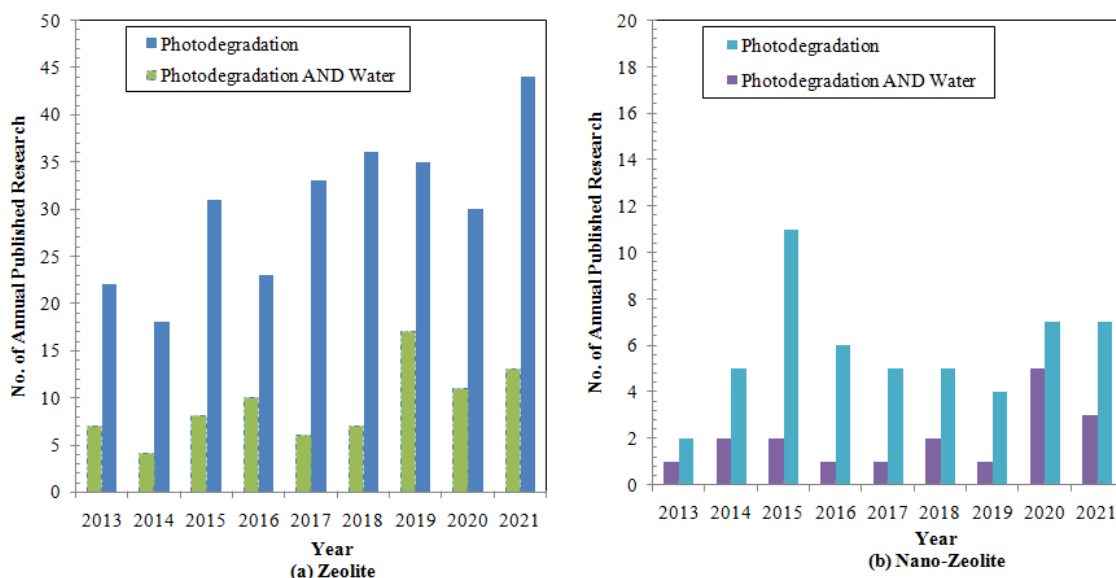


**Figure 7.** Annual distribution of the research that addressed the application of (a) zeolites; (b) nano-zeolites in photo-degradation and photo-degradation in water.

### 3.1. Testing Scheme to Optimize the Photo-Catalytic Degradation Applications

In general, the testing schemes for evaluating the performance of photo-catalytic composites include material characterization, and operational condition optimization. The aim of the characterization step is to identify the chemical and physical properties of benefits to the photo-catalytic degradation process, where both the sorption and photo-catalytic degradation related properties are identified. Thus, in addition to the characterization methods mentioned in Section 2.1, the optical properties of the photo-catalytic composite are widely employed. In this context, the diffuse reflectance and the photoluminescence spectroscopy are used to evaluate the structural changes in the composite during different treatments, calculate the band gap value, and identify the defects in the structures [133–137]. In Velásquez et al. [137], erosion, reusability, and composite degradation tests were conducted to assess the effect of mixing either mechanical or sonication on the polymer composite stability, degradation efficiency behavior under repeated reusability, and composite degradation resistance under prolonged exposure to the radiation. It should be noted that the reusability is associated with efficiency reduction due to the sorption of the degradation products on the zeolite surface [138]. Operational conditions optimizations could be conducted via the OFAT or MVT technique to identify the optimum catalyst composite mass ( $m$ , g), optimum catalyst to support ratio, contaminated solution volume ( $V$ , L) and pH, initial contaminant concentration ( $C_0$ , mmol/L), contact time ( $t_{eq}$ , min), and effect of the support.

### 3.2. Batch Investigations

Batch investigations of photo-catalytic composites are employed to design the photo-degradation process. In these investigations, certain mass of the photo-catalytic composite ( $m$ , g) is mixed with a certain volume of the contaminated solution ( $V$ , L) of specified contaminant concentration ( $C_0$ , mmol/L) and pH at specified mixing velocity for a certain

period of time under specified illumination conditions. Then, the solid/liquid suspension is separated and the contaminant concentration ( $C_t$ , mmol/L) in the solution is measured using a suitable analytical technique. The degradation efficiency (Deg, %) is determined using the following equation:

$$\text{Deg.}\% = \left( \frac{C_o - C_t}{C_o} \right) \times 100 \quad (4)$$

The experiments are usually conducted under dark conditions to ensure the achievement of the sorption equilibrium and then illumination is turned on to allow a clear identification of the photo-degradation.

Kinetic studies are conducted to allow the calculations of the operational time and rate constants of the degradation reactions. In this respect, the sorption kinetics models PFO, PSO, and IPM are widely used to investigate the sorption and diffusion step in the process. Langmuir–Hinshelwood (LH), and first order (FO) are widely used to analyze the photo-degradation kinetics, and the features of each model are listed in Table 7 [139,140]. Different efforts were directed to provide mechanistic models that could be used to better represent the reaction kinetics, estimating the controlling steps, and obtaining a precise value for the rate constants [140–144]. Equilibrium investigations in terms of varying the initial contaminant concentration in the aqueous solution are usually modeled using the sorption equilibrium models [139,140,145]. It should be noted that, for sunlight driven processes, the variation of the solar intensity with time and reactor depth should be considered during the design of the process.

**Table 7.** Models used in analyzing the photo-degradation kinetics.

Model	Equation	Model Features
LH	Linear: $\ln\left(\frac{C_o}{C_o-C}\right) = -\frac{k_{ad}k_{LH}t}{(C_o-C)} - k_{ad}$	The model assumes that the rate of the photo-degradation reaction proportional to the fraction of the surface by the contaminant, It assumes that the available contaminants on the surface are sorbed following the Langmuir monolayer model,
	Non-linear: $C = C_o e^{-k_{ad}(k_{LH}t + C_o - C)}$	The model does not consider the reactions of the intermediates, $K_x$ the rate constant for sorption ( $x = ad$ ) and photo-degradation ( $x = LH$ )
FO	Linear : $\ln\left(\frac{C_o}{C_o-C}\right) = -k_f t$	Assumes that the overall degradation process is a first order reaction valid for diluted solutions $K_f$ is the apparent first order rate constant
	Non – linear : $C = C_o e^{-k_f t}$	

The reusability of the photo-catalytic composite is tested by repeating the batch experiment under optimum degradation conditions using fresh contaminant concentration at each cycle. The composite is re-used after drying at specified temperature for a fixed amount of time. The regeneration ability is tested after regenerating the surface of the materials using chemicals; then, the batch experiments are repeated.

### 3.3. Applications in Organic Contaminant Degradation

The indexed research directed to explore the feasibility of using nano-zeolite in the preparation of photo-catalytic composite for the degradation of organic contaminants are listed in Table 8 [146–154]. The following concluding remarks could be drawn:

- Most of the conducted research utilized natural CLP grounded to the nano-scale, and limited research utilized synthetic ZSM-5 nano zeolites for their applications in the preparation of photo-catalytic composites.
- The composites included metal oxides e.g., ZnO, CuO, FeO, NiO, and metal sulfide, e.g., ZnS, NiS, CuS, and PbS.
- Most of the conducted experiments employed a single contaminant solution, where solutions of model organic contaminant, e.g., 4-Nitrophenol, Dyes, e.g., Rhodamine B,

Methylene blue, personal care products and pharmaceutical compounds, e.g., Metronidazole, Tetracycline, Cefuroxime, Benzophenone. Real effluent, i.e., fish pond water, was only used in one research.

- The tested photo-catalytic composite dosage was in the range (0.025–3), where, in some studies, oxidizer, e.g.,  $H_2O_2$ , was supplemented to the contaminant solution.

**Table 8.** Results of the applications of nano-zeolite composite for photo-catalytic degradation of organic contaminants.

Cont.	Nano-Zeolite				Illumination Source	m/Vg/L	Optimum Conditions			Model	Reuse	Ref.
	Type	Size, nm	Composite	Preparation			$C_{or}$ , ppm	pH	$t_{eq}$ , min			
MB	CLP	50	ZnO	Natural	Fluorescence lamp, 60 W	0.25	10	-	50	FO	4	[146]
MB	ZSM-5	-	ZnO	HT-chemical	UV-Mercury lamp, 500 W	0.2	50	-	30	FO	6	[147]
TC	CLP	100	FeO	Natural	Hg lamp, 30 W	0.2	-	4.3	200	FO	6	[148]
CF	CLP	10–70	NiO	Natural	Hg lamp, 35 W	0.025	-	4.3	200	LH	-	[149]
FP	CLP	-	FeO-ZnO	Natural	Sunlight	0.1	-	8.3	140	-	5	[150]
4-NP	CLP	52	NiS/PbS	Natural	Hg lamp, 30 W	0.5	-	7.5	200	FO	-	[151]
MB	CLP	100	CuO	Natural	Hg lamp, 75 W	0.2	7	5.9	180	FO	-	[152]
MZ	CLP	30	ZnS/NiS	Natural	Hg lamp, 35 W	3	4	3	150	-	-	[153] MVT
BP	CLP	-	ZnO/CuO	Natural	2 Hg lamp, each 35 W	0.12	30	7.5	300	FO	5	[154]
			ZnS/CuS			0.1	30	7.5			5	

Note: RB = Rhodamine B. (TC) = Tetracycline. (CF) = Cefuroxime. Fp = Filtered Fish Pond Wastewater. 4-NP = 4-Nitrophenol. MZ = Metronidazole. BP = Benzophenone.

The examination of the listed data in Table 8 shows that most of the analyses were conducted using the linear form of the FO model, where the experiments were conducted after reaching the sorption–desorption equilibrium. The analysis of the integrated process of sorption and diffusion, photo-catalytic degradation, and desorption of the degradation products were not conducted. Only one research work tested the photo-degradation under sunlight, and the rest of the published work employed lamps as an illumination source.

#### 4. Advances in Nano-Zeolite Applications in Membrane Separation

Contaminants and/or salt removal from the water and wastewater are achieved in membrane technology by using a barrier that allows selective transport of certain molecules, ions, or particles under driving force [37]. The driving force could be pressure, concentration, or potential gradients. This barrier comprises two-layers or more, where the upper layer is a thin denser layer (active layer) that is overlaying more porous and thicker substrates. Two categories of materials are widely used to construct the membrane namely: polymer and ceramic. The membrane technology is usually classified based on the pore size of the membrane into microfiltration (MF), ultra-filtration (UF), nano-filtration (NF), and reverse osmosis (RO). Compared to polymeric membranes, ceramic membranes are characterized by their higher porosity, higher hydrophilicity, and better chemical, mechanical, thermal, and biological stabilities which are translated to better hydraulic performance, lower fouling rates, and longer service time. Subsequently, ceramic membranes are applied in all membrane classes, with wider applications in MF and UF [155]. Alumina, silica, zeolite, tetania, and zirconia are five principal materials in ceramic membrane preparation. In particular, zeolites are used to form the active layer in MF, UF, and RO with relatively limited utilization as a substrate. Compared to other ceramic membrane materials, zeolites have the second highest hydrophilicity and unique pore structures, but their chemical and thermal stabilities are not advantageous [155]. Mixed matrix membranes (MMM) are formed from Nano-Polymer Composites (NPC) to overcome

the drawbacks of the polymeric membranes using inorganic filler or additives [37,156,157]. There are two configurations that are widely used in this context, namely: conventional PNC, and thin film composites (TFC) deposited on the PNC surface [158]. The application of adsorptive membranes, adsorption-membranes hybrid treatment system, and nano-fibrous membranes using electrospinning in water treatment were reviewed [159–161]. The analysis of the research indexed in the Scopus database was conducted using the keywords zeolite and nano-zeolite combined with the keywords treatment and water; the results are illustrated in Figure 8a,b. The annual number of indexed research focused on the study of zeolites was considerably larger than those studying nano-zeolites. The research that assesses the potential use of zeolites in membrane application for water treatment is nearly two thirds of those used for the treatment. On the other hand, almost all the studies that addressed the nano-zeolites directed for its use in membranes were focused on water treatment. The research trends are slightly increased over the studied time.

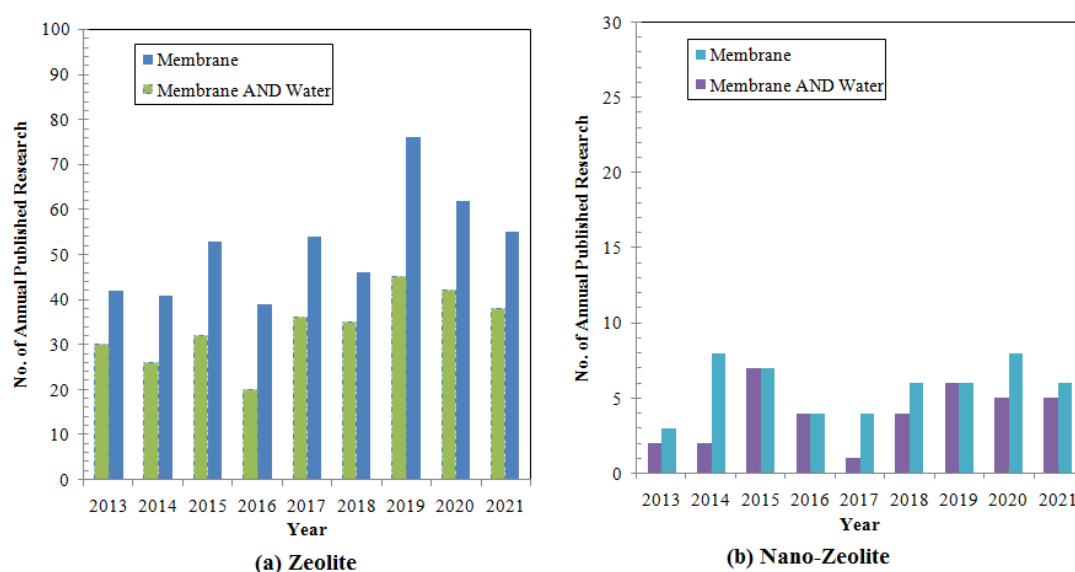


**Figure 8.** Annual distribution of the research that addressed the application of (a) zeolites; (b) nano-zeolites in membrane and membrane in water.

#### 4.1. Testing Scheme to Optimize the Membrane Applications

As in the other applications, the testing schemes for evaluating the performance of nano-zeolites containing membranes include material characterization and operational conditions optimization. Material characterizations are conducted to identify the membrane composition and its physical properties, where the particle size, pore structure, morphology and surface properties, chemical composition, and crystallinity are identified as mentioned in Section 2.1. In addition, the hydrophilicity of the membrane is characterized using a water contact angle technique. Moreover, the stress–strain behavior of the membrane is evaluated to have insights on the reliability of the designed membrane. Fouling resistance is usually determined by applying repeated cycles of treatment–backwash and or chemical treatment. Bio fouling resistance is usually quantified by assessing the initial bacterial attachment to the membrane and the inhabitation of the micro-organisms' growth, e.g., *E-coli*, *P. aeruginosa* LB, on the membrane surface. OFAT is usually used to assess the performance of the membrane and optimize the operational conditions as will be presented in the next subsection.

#### 4.2. Identification of Membrane Performance

Batch and continuous experiments are conducted; the batch experiments give an indication on the sorption characteristics for adsorptive membranes. In these experiments, the procedure for batch sorption is adopted and sorption characteristics are identified [162,163].

In continuous experiments, the contaminated solution is flowing through the membrane by the action of the driving force. In pressure driven membrane applications, the system is subjected to a specified pressure using a suitable pump. Feed of contaminated solution of concentration ( $C_f$ , mg/L) is pumped through the membrane and the contaminant concentration in the permeate is measured ( $C_p$ , mg/L). The membrane efficiency is determined in terms of contaminant rejection ( $R$ , %) using the following equation:

$$R = 1 - \frac{C_p}{C_f} \times 100 \quad (5)$$

The permeate flux ( $J_w$ , L/(m<sup>2</sup>.h)) is determined from the ratio between the permeated volume in a given time ( $V(t)$ , l/h), and the membrane area ( $A$ , m<sup>2</sup>) is as follows:

$$J_w = \frac{V(t)}{A} \quad (6)$$

Three parameters could be used to compare the fouling resistance, which is the flux recovery ratio (FRR), which is the percentage of the permeated pure water after repeated filtration cycles to that before the cycles permeate, i.e.,  $J_{wn}$  and  $J_{w1}$ , respectively [164]:

$$FRR (\%) = \frac{J_{wn}}{J_{w1}} \times 100 \quad (7)$$

Total fouling ( $R_t$ , %) and irreversible fouling ( $R_{ir}$ , %) could be assessed by finding the percentage of the change in water flux after to backwash ( $J_{wb}$ ) and chemical treatment ( $J_{wc}$ ) according to the following equations [165]:

$$R_t (\%) = \frac{J_{wb} - J_t}{J_{wb}} \times 100 \quad (8)$$

$$R_{ir} (\%) = \frac{J_{wb} - J_{wc}}{J_{wb}} \times 100 \quad (9)$$

#### 4.3. The Membrane Investigations

The results of indexed research that addressed the application of nano-zeolite in membrane separation are presented in Table 9 [165–171]. Different types of nano-zeolites and modified nano-Zeolites were tested in a continuous testing scheme following the OFAT technique. The research addressed the removal of metal and organic pollutants, i.e., dyes, simulated waste effluent, and oil. The research mainly used the pressure as the driving force, except for one research work that utilized potential difference. The following concluding remarks could be drawn:

- Zeolite-Y, Na-X, FAU, Na-A, and beta were used as an active layer in the membrane composite, via depositing a thin film on the substrate or embedding onto the membrane matrix;
- Different modifications for the nano-zeolites were proposed including the addition of metals, e.g., Cu, oxides, e.g., TiO<sub>2</sub>, and organic modification, e.g., D-tyrosine. These modifications were used to increase the fouling resistance.
- The applications were restricted to MF, UF, and NF, despite there are some research studies that tested the use of nano-zeolite in membrane applications for dehydration of different products using RO and forward osmosis, but these membrane types were not tested for wastewater treatment.



**Table 9.** Application of nano-zeolite in membrane separations.

Cont.	Membrane			Contact Angle, °	Optimum Conditions				Fouling	Ref.
	Active Layer	Substrate	Type		C <sub>o</sub> , ppm	Flux, lm <sup>2</sup> /h	R, %	Pressure, bar		
CV	Zeolite-Y	CNS	UF-conductive	40	20	210	100	@3 volte	-	[165]
Engine Oil	Beta	CA	MF	67.7	2%	-	97	Vacuum-	-	[166]
Oil	Zeolite NaX-TiO <sub>2</sub>	PES	UF	-	-	-	-	-	-	[167]
TPH	Zeolite -NaA	Polyaniline	NF	-	35.1-78.0	96.99	77.79	5	-	[168]
Paper mill effluent	Cu-Zeolite	PES	UF	73.4-74.8	COD = 1840, PH = 7.6, BOD = 660, So4 = 205, Cl = 340	38.9	COD = 89 BOD = 90.5	4.14	Fouling	[164]
Syenthctic wastewater	FAU-D-tyrosine	NF270	NF	20	-	-	-	-	Bio fouling	[169]
As	Zeolite	Chitosan	-	74.2-59.2	1000	-	94	-	-	[170]
Ni	Zeolite-Na-X	PSf	UF	67	500	21	91	1	-	[171]
Pb						21	42			

Note: TPH = Total Petroleum Hydrocarbon. CNS = Carbon Nanostructure. CA = Cellulose acetate. PES = Polyethersulfone. PSf = Polysulfone.

## 5. Conclusions

The applications of nano-zeolite in water and wastewater treatment were reviewed in this work, where the application of zeolites in this field was introduced, and zeolites structures and their properties and recent trends in the preparation of zeolites were overviewed. The various applications of the nano-zeolites in the field were addressed by focusing on the applications of nano-zeolite in ion-exchange/sorption, photo-degradation, and membrane separation. In this respect, in depth analysis of the variation of the annual research indexed in Scopus database was performed for each application to have insights into the trends of the scientific interest in this field. The characterization schemes, experimental investigations, and theoretical analysis of the data were presented. Finally, the results of recent research were summarized, analyzed, and concluding remarks were drawn for each application. Based on these concluding remarks, some gaps in this innovative field of study were identified as follows:

- Despite it being found that the use of nano-zeolite has enhanced the performance of the treatment process and subsequently can reduce the size and land requirement of the wastewater treatment plant, there is a need to consider the reduction of the materials footprints; this could be achieved by following greener nano-zeolite preparation techniques, i.e., use of bio-materials and wastes as sources for the preparation, use of biosolvent, and low temperature processes.
- Batch experiment for nano-zeolite applications in ion exchange/sorption process is a major research field with the highest number of published papers. This forms a database that can assist with the wide-scale application of several types of nano-zeolites for the removal of different contaminants including radioactive, metal, and organic. Research that assesses the continuous application of nano-zeolites in this field is very limited, where there is a need to assess the hydraulic and sorptive performance of this type of application.
- Despite nano-zeolite being able to be modified to act as anion exchanger/sorbent, these research investigations are very limited. Moreover, the research that includes the application of complicated solutions is missing, i.e., real wastewater. Finally, the application of nano-zeolites for the treatment of corrosive wastewater stream is not sufficiently addressed.
- For photo-degradation applications, there is a need to consider the application on complex/ real wastewater effluent, where the research only focuses on the use of a single contaminant solution.

- For membrane separation, the application of nano-zeolite in RO and forward osmosis is missing in the field of water and wastewater treatment.
- Hierarchical and 2D zeolites were not investigated yet in any application related to water and wastewater treatment.
- For all the presented applications, neither the cost analysis for the preparation and application of nano-zeolite in water and wastewater treatment nor the pilot scale applications were addressed. These types of investigations can help in paving the way toward the wide application of these materials in the industry.
- For each application, the research that addressed the life cycle management of nano-zeolite is missing. In particular, clear assessment of the end of life cycle management options for the exhausted nano-materials should be conducted.

**Author Contributions:** Conceptualization, R.O.A.R.; methodology, R.O.A.R.; resources, R.O.A.R. and Y.-T.H.; writing—review and editing, R.O.A.R., A.M.E.-K. and Y.-T.H. All authors have read and agreed to the published version of the manuscript.

**Funding:** This research received no external funding.

**Institutional Review Board Statement:** Not applicable.

**Informed Consent Statement:** Not applicable.

**Data Availability Statement:** Not applicable.

**Conflicts of Interest:** The authors declare no conflict of interest.

## References

1. Tortajada, C. Contributions of recycled wastewater to clean water and sanitation Sustainable Development Goals. *NPJ Clean Water* **2020**, *3*, 22. [\[CrossRef\]](#)
2. Abdel Rahman, R.O.; Hung, Y.-T. Application of Ionizing Radiation in Wastewater Treatment: An Overview. *Water* **2020**, *12*, 19. [\[CrossRef\]](#)
3. Guth, J.L.; Kessler, H. Synthesis of Aluminosilicate Zeolites and Related Silica-Based Materials. In *Catalysis and Zeolites Fundamentals and Applications*; Weitkamp, J., Puppe, L., Eds.; Springer: Berlin/Heidelberg, Germany, 1999; pp. 1–52.
4. Jha, B.; Singh, D.N. Basics of zeolites. In *Fly Ash Zeolites*; Springer: Singapore, 2016; pp. 5–31.
5. Millini, R.; Belluss, G. Zeolite Science and Perspectives. In *Zeolites in Catalysis: Properties and Applications*; Cejka, J., Morris, R.E., Nachtigall, P., Eds.; RSC Catalysis Series No. 28; The Royal Society of Chemistry: Cambridge, UK, 2017.
6. Tsai, Y.L.; Huang, E.; Li, Y.H.; Hung, H.T.; Jiang, J.H.; Liu, T.C.; Fang, J.N.; Chen, H.F. Raman Spectroscopic Characteristics of Zeolite Group Minerals. *Minerals* **2021**, *11*, 167. [\[CrossRef\]](#)
7. Abdel Rahman, R.O.; Metwally, S.S.; El-Kamash, A.M. Life Cycle of Ion Exchangers in Nuclear Industry: Application and Management of Spent Exchangers. In *Handbook of Ecomaterials*; Martínez, L., Kharissova, O., Kharisov, B., Eds.; Springer: Cham, Switzerland, 2019; Volume 5, pp. 3709–3732. [\[CrossRef\]](#)
8. Byrappa, K.; Yoshimura, M. *Handbook of Hydrothermal Technology*; Noyes Publications: Park Ridge, IL, USA, 2001.
9. Abdel Rahman, R.O.; Ojovan, M.I. Application of nano-materials in radioactive waste management. In *Environmental Science and Engineering*; Zhang, T.C., Gurjar, B.R., Govil, J.N., Eds.; Studium Press, LLC: New York, NY, USA, 2017; Volume 10, pp. 361–378.
10. Abdel Rahman, R.O.; Ibrahim, H.A.; Abdel Monem, N.M. Long-term performance of Zeolite Na A-X blend as backfill material in near surface disposal vault. *Chem. Eng. J.* **2009**, *149*, 143–152. [\[CrossRef\]](#)
11. Abdel Rahman, R.O.; Ibrahim, H.A.; Hanafy, M.; Abdel Monem, N.M. Assessment of synthetic zeolite NaA-X as sorbing barrier for strontium in a radioactive disposal facility. *Chem. Eng. J.* **2010**, *157*, 100–112. [\[CrossRef\]](#)
12. El-Naggar, M.R.; El-Kamash, A.M.; El-Dessouky, M.I.; Ghonaim, A.K. Two-step method for preparation of NaA-X zeolite blend from fly ash for removal of cesium ions. *J. Hazard. Mater.* **2008**, *154*, 963–972. [\[CrossRef\]](#)
13. Ames, L.L., Jr. Synthesis of a clinoptilolite-like zeolite. *Am. Miner.* **1963**, *48*, 1374–1381.
14. Jacobs, P.A.; Flanigen, E.M.; Jansen, J.C.; van Bekkum, H. *Introduction to Zeolite Science and Practice*; Elsevier: Amsterdam, The Netherlands, 2001.
15. Abdel Moamen, O.A.; Ismail, I.M.; Abdel Monem, N.M.; Abdel Rahman, R.O. Factorial design analysis for optimizing the removal of cesium and strontium ions on synthetic nano-sized zeolites. *J. Taiwan Inst. Chem. Eng.* **2015**, *55*, 133–144. [\[CrossRef\]](#)
16. Gil, A.; Korili, S.A. Management and valorization of aluminum saline slags: Current status and future trends. *Chem. Eng. J.* **2016**, *289*, 74–84. [\[CrossRef\]](#)
17. Ma, L.J.; Han, L.N.; Chen, S.; Hu, J.L.; Chang, L.P.; Bao, W.R.; Wang, J. Rapid synthesis of magnetic zeolite materials from fly ash and iron-containing wastes using supercritical water for elemental mercury removal from flue gas. *Fuel Process. Technol.* **2019**, *189*, 39–48. [\[CrossRef\]](#)

18. Kuroki, S.; Hashishin, T.; Morikawa, T.; Yamashita, K.; Matsuda, M. Selective synthesis of zeolites A and X from two industrial wastes: Crushed stone powder and aluminum ash. *J. Environ. Manag.* **2019**, *231*, 749–756. [\[CrossRef\]](#) [\[PubMed\]](#)
19. Yoldi, M.; Fuentes-Ordoñez, E.G.; Korili, S.A.; Gil, A. Zeolite synthesis from industrial wastes. *Microporous Mesoporous Mater.* **2019**, *287*, 183–191. [\[CrossRef\]](#)
20. Gao, W.; Amoo, C.C.; Zhang, G.; Javed, M.; Mazonde, B.; Lu, C.; Yang, R.; Xing, C.; Tsubaki, N. Insight into solvent-free synthesis of MOR zeolite and its laboratory scale production. *Microporous Mesoporous Mater.* **2019**, *280*, 187–194. [\[CrossRef\]](#)
21. Mei, J.; Duan, A.; Wang, X. A Brief Review on Solvent-Free Synthesis of Zeolites. *Materials* **2021**, *14*, 788. [\[CrossRef\]](#)
22. Li, K.; Valla, J.; Garcia-Martinez, J. Realizing the Commercial Potential of Hierarchical Zeolites: New Opportunities in Catalytic Cracking. *ChemCatChem* **2014**, *6*, 46–66. [\[CrossRef\]](#)
23. Feliczak-Guzik, A. Hierarchical zeolites: Synthesis and catalytic properties. *Microporous Mesoporous Mater.* **2018**, *259*, 33–45. [\[CrossRef\]](#)
24. Mintova, S.; Gilson, J.P.; Valtchev, V. Advances in nanosized Zeolites. *Nanoscale* **2013**, *5*, 6693. [\[CrossRef\]](#)
25. Pan, T.; Wu, Z.; Yip, A.C.K. Advances in the Green Synthesis of Microporous and Hierarchical Zeolites: A Short Review. *Catalysts* **2019**, *9*, 274. [\[CrossRef\]](#)
26. Cao, Z.; Zeng, S.; Xu, Z.; Arvanitis, A.; Yang, S.; Gu, X.; Dong, J. Ultrathin ZSM-5 zeolite nanosheet laminated membrane for high-flux desalination of concentrated brines. *Sci. Adv.* **2018**, *4*, eaau8634. [\[CrossRef\]](#)
27. Rehman, A.u.; Arepalli, D.; Alam, S.F.; Kim, M.-Z.; Choi, J.; Cho, C.H. Two-Dimensional MFI Zeolite Nanosheets Exfoliated by Surfactant Assisted Solution Process. *Nanomaterials* **2021**, *11*, 2327. [\[CrossRef\]](#)
28. Abdel Rahman, R.O.; Abdel Moamen, O.A.; Hanafy, M.; Abdel Monem, N.M. Preliminary investigation of zinc transport through zeolite-X barrier: Linear isotherm assumption. *Chem. Eng. J.* **2012**, *185–186*, 61–70. [\[CrossRef\]](#)
29. Choi, H.J.; Yu, S.W.; Kim, K.H. Efficient use of Mg-modified zeolite in the treatment of aqueous solution contaminated with heavy metal toxic ions. *J. Taiwan Inst. Chem. Eng.* **2016**, *63*, 482–489. [\[CrossRef\]](#)
30. Tran, H.N.; Viet, P.V.; Chao, H.P. Surfactant modified zeolite as amphiphilic and dual-electronic adsorbent for removal of cationic and oxyanionic metal ions and organic compounds. *Ecotoxicol. Environ. Saf.* **2018**, *147*, 55–63. [\[CrossRef\]](#) [\[PubMed\]](#)
31. Rad, L.R.; Anbia, M. Zeolite-based composites for the adsorption of toxic matters from water: A review. *J. Environ. Chem. Eng.* **2021**, *9*, 106088.
32. Rodríguez-Iznaga, I.; Rodríguez-Fuentes, G.; Petranovskii, V. Ammonium modified natural clinoptilolite to remove manganese, cobalt and nickel ions from wastewater: Favorable conditions to the modification and selectivity to the cations. *Microporous Mesoporous Mater.* **2018**, *255*, 200–210. [\[CrossRef\]](#)
33. Zhang, H.; Li, A.; Zhang, W.; Shuang, C. Combination of Na-modified Zeolite and anion exchange resin for advanced treatment of a high ammonia-nitrogen content municipal effluent. *J. Colloid Interface Sci.* **2016**, *468*, 128–135. [\[CrossRef\]](#)
34. Wen, J.; Dong, H.; Zeng, G. Application of zeolite in removing salinity/sodicity from wastewater: A review of mechanisms, challenges and opportunities. *J. Clean. Prod.* **2018**, *197*, 1435–1446. [\[CrossRef\]](#)
35. Jiménez-Reyes, M.; Almazán-Sánchez, P.T.; Solache-Ríos, M. Radioactive waste treatments by using zeolites. A short review. *J. Environ. Radioact.* **2021**, *233*, 106610. [\[CrossRef\]](#)
36. Fatima, H.; Djamel, N.; Samira, A.; Mahfoud, B. Modelling and adsorption studies of removal uranium (VI) ions on synthesised zeolite NaY. *Desalin. Water Treat.* **2013**, *51*, 5583–5591. [\[CrossRef\]](#)
37. Abdel Rahman, R.O.; Abdel Moamen, O.A.; El-Masry, E.H. Life cycle of polymer nanocomposites matrices in hazardous waste management. In *Handbook of Polymer and Ceramic Nanotechnology*; Hussain, C.M., Thomas, S., Eds.; Springer Nature: Cham, Switzerland, 2021; pp. 1603–1625. [\[CrossRef\]](#)
38. Abdel Rahman, R.O.; Abdel Moamen, O.A.; Abdelmonem, N.; Ismail, I.M. Optimizing the removal of strontium and cesium ions from binary solutions on magnetic nano-zeolite using response surface methodology (RSM) and artificial neural network (ANN). *Environ. Res.* **2019**, *173*, 397–410. [\[CrossRef\]](#)
39. Abdel Rahman, R.O.; Ojovan, M.I. Toward Sustainable Cementitious Radioactive Waste Forms: Immobilization of Problematic Operational Wastes. *Sustainability* **2021**, *13*, 11992. [\[CrossRef\]](#)
40. Dyer, A.; Hriljac, J.; Evans, N.; Stokes, I.; Rand, P.; Kellet, S.; Harjula, R.; Moller, T.; Maher, Z.; Heatlie-Branson, R.; et al. The use of columns of the zeolite clinoptilolite in the remediation of aqueous nuclear waste streams. *J. Radioanal. Nucl. Chem.* **2018**, *318*, 2473–2491. [\[CrossRef\]](#) [\[PubMed\]](#)
41. Osmanlioglu, E. Treatment of radioactive liquid waste by sorption on natural zeolite in Turkey. *J. Hazard. Mater.* **2006**, *137*, 332–335. [\[CrossRef\]](#)
42. El-Dessouky, M.I.; El-Kamash, A.M.; El-Sourougy, M.R.; Aly, H.F. Simulation of Zeolite Fixed Bed Columns Used for Treatment of Liquid Radioactive Wastes. *Radiochem. Acta* **2000**, *88*, 879–884. [\[CrossRef\]](#)
43. El-Kamash, A.M.; Zaki, A.A.; El Geleel, M.A. Modeling Batch Kinetics and Thermodynamics of Zinc and Cadmium Ions Removal from Waste Solution Using Synthetic Zeolite A. *J. Hazard. Mater.* **2005**, *127*, 211–220. [\[CrossRef\]](#)
44. El-Rahman, K.M.A.; El-Kamash, A.M.; El-Sourougy, M.R.; Abdel-Moniem, N.M. Thermodynamic Modeling for the Removal of Cs<sup>+</sup>, Sr<sup>2+</sup>, Ca<sup>2+</sup>, and Mg<sup>2+</sup> Ions from Aqueous Waste Solution Using Zeolite A. *J. Radioanal. Nucl. Chem.* **2006**, *268*, 221–230. [\[CrossRef\]](#)
45. Fang, X.-H.; Fang, F.; Lu, C.-H.; Zheng, L. Removal of Cs<sup>+</sup>, Sr<sup>2+</sup>, and Co<sup>2+</sup> ions from the mixture of organics and suspended solids aqueous solutions by zeolites. *Nucl. Eng. Technol.* **2017**, *49*, 556–561. [\[CrossRef\]](#)

46. El-Kamash, A.M. Evaluation of zeolite A for the sorptive removal of  $\text{Cs}^+$  and  $\text{Sr}^{2+}$  ions from aqueous solutions using batch and fixed bed column operations. *J. Hazard. Mater.* **2008**, *151*, 432–445. [\[CrossRef\]](#)
47. Abd El-Rahman, K.M.; El-Sourougy, M.R.; Abdel-Monem, N.M.; Ismail, I.M. Modeling the Sorption Kinetics of Cesium and Strontium Ions on Zeolite A. *J. Nucl. Radiochem. Sci.* **2006**, *7*, 21–27. [\[CrossRef\]](#)
48. Baek, W.; Ha, S.; Hong, S.; Kim, S.; Kim, Y. Cation exchange of cesium and cation selectivity of natural zeolites: Chabazite, stilbite, and heulandite. *Microporous Mesoporous Mater.* **2018**, *264*, 159–166. [\[CrossRef\]](#)
49. Lihareva, N.; Petrov, O.; Dimowa, L.; Tzvetanova, Y.; Piroeva, I.; Ublekov, F.; Nikolov, A. Ion exchange of  $\text{Cs}^+$  and  $\text{Sr}^{2+}$  by natural clinoptilolite from bi-cationic solutions and XRD control of their structural positioning. *J. Radioanal. Nucl. Chem.* **2020**, *323*, 1093–1102. [\[CrossRef\]](#)
50. Mosai, A.K.; Chimuka, L.; Cukrowska, E.M.; Kotzé, I.A.; Tutu, H. The recovery of rare earth elements (REEs) from aqueous solutions using natural zeolite and bentonite. *Water Air Soil Pollut.* **2019**, *230*, 188. [\[CrossRef\]](#)
51. Chen, Z.; Lu, S. Investigation of the effect of pH, ionic strength, foreign ions, temperature, soil humic substances on the sorption of  $^{152}\text{Eu}$  and  $^{154}\text{Eu}$  (III) onto NKF-6 zeolite. *J. Radioanal. Nucl. Chem.* **2016**, *309*, 717–728. [\[CrossRef\]](#)
52. Abdi, M.R.; Shakur, H.R.; Saraee, K.R.E.; Sadeghi, M. Effective removal of uranium ions from drinking water using CuO/X zeolite based nanocomposites: Effects of nano concentration and cation exchange. *J. Radioanal. Nucl. Chem.* **2014**, *300*, 1217–1225. [\[CrossRef\]](#)
53. Lazaridis, N.K.; Karapantsios, T.D.; Georgantas, D. Kinetic analysis for the removal of a reactive dye from aqueous solution onto hydrotalcite by adsorption. *Water Res.* **2003**, *37*, 3023–3033. [\[CrossRef\]](#)
54. Krajňák, A.; Viglašová, E.; Galamboš, M.; Krivosudský, L. Kinetics, thermodynamics and isotherm parameters of uranium (VI) adsorption on natural and HDTMA-intercalated bentonite and zeolite. *Desalin. Water Treat.* **2018**, *127*, 272–281. [\[CrossRef\]](#)
55. Al-Shaybe, M.; Khalili, F. Adsorption of thorium (IV) and uranium (VI) by Tulul al-shabba zeolitic tuff. *Jordan J. Earth Environ. Sci.* **2009**, *2*, 108–109.
56. Nyembe, D.W.; Mamba, B.B.; Mulaba-Bafubandi, A.F. The Effect of Si and Fe Impurities on the Removal of  $\text{Cu}^{2+}$  and  $\text{Co}^{2+}$  from Co/Cu aqueous solutions using natural clinoptilolite as an ion-exchanger. *Desalin. Water Treat.* **2010**, *21*, 335–345. [\[CrossRef\]](#)
57. Rodríguez, A.; S'aez, P.; Díez, E.; Gómez, J.M.; García, J.; Bernabé, I. Highly efficient low-cost zeolite for cobalt removal from aqueous solutions: Characterization and performance. *Am. Inst. Chem. Eng. Environ. Prog.* **2018**, *38*, S352–S365. [\[CrossRef\]](#)
58. Irannajad, M.; Haghighi, H.K. Removal of  $\text{Co}^{2+}$ ,  $\text{Ni}^{2+}$ , and  $\text{Pb}^{2+}$  by manganese oxide-coated zeolite: Equilibrium, thermodynamics, and kinetics studies. *Clay Miner.* **2017**, *65*, 52–62. [\[CrossRef\]](#)
59. Liang, J.; Li, J.; Li, X.; Liu, K.; Wu, L.; Shan, G. The sorption behavior of CHA-type zeolite for removing radioactive strontium from aqueous solutions. *Sep. Purif. Technol.* **2020**, *230*, 115874. [\[CrossRef\]](#)
60. Hassan, R.S.; Abass, M.R.; Eid, M.A.; Abdel-Galil, E.A. Sorption of some radionuclides from liquid waste solutions using anionic clay hydrotalcite sorbent. *Appl. Radiat. Isot.* **2021**, *178*, 109985. [\[CrossRef\]](#)
61. Abdel Moamen, O.A.; Ibrahim, H.A.; Abdelmonem, N.; Ismail, I.M. Thermodynamic analysis for the sorptive removal of cesium and strontium ions onto synthesized magnetic nano Zeolite. *Microporous Mesoporous Mater.* **2016**, *223*, 187–195. [\[CrossRef\]](#)
62. Faghihian, H.; Moayed, M.; Firooz, A.; Irvan, M. Synthesis of a novel magnetic zeolite nanocomposite for removal of  $\text{Cs}^+$  and  $\text{Sr}^{2+}$  from aqueous solution: Kinetic, equilibrium, and thermodynamic studies. *J. Colloid Interface Sci.* **2013**, *393*, 445–451. [\[CrossRef\]](#)
63. Sharma, P.; Tomar, R. Sorption behaviour of nanocrystalline MOR type zeolite for Th(IV) and Eu(III) removal from aqueous waste by batch treatment. *J. Colloid Interface Sci.* **2011**, *362*, 144–156. [\[CrossRef\]](#)
64. Lee, K.Y.; Kim, K.W.; Park, M.; Kim, J.; Oh, M.; Lee, E.H.; Chung, D.Y.; Moon, J.K. Novel application of nanozeolite for radioactive cesium removal from high-salt wastewater. *Water Res.* **2016**, *95*, 134–141. [\[CrossRef\]](#)
65. Talebi, M.; Abbasizadeh, S.; Keshtkar, A.R. Evaluation of Single and Simultaneous Thorium and Uranium Sorption from Water Systems by an Electrospun PVA/SA/PEO/HZSM5 Nanofiber. *Process Saf. Environ. Prot.* **2017**, *109*, 340–356. [\[CrossRef\]](#)
66. Zahakifar, F.; Keshtkar, A.R.; Talebi, M. Performance evaluation of sodium alginate/polyvinyl alcohol/ polyethylene oxide/ ZSM5 zeolite hybrid adsorbent for ion uptake from aqueous solutions: A case study of thorium (IV). *J. Radioanal. Nucl. Chem.* **2021**, *327*, 65–72. [\[CrossRef\]](#)
67. Murukutti, M.K.; Jena, H. Synthesis of nano-crystalline zeolite-A and zeolite-X from Indian coal fly ash, its characterization and performance evaluation for the removal of  $\text{Cs}^+$  and  $\text{Sr}^{2+}$  from simulated nuclear waste. *J. Hazard. Mater.* **2022**, *423*, 127085. [\[CrossRef\]](#) [\[PubMed\]](#)
68. Paris, E.C.; Malafatti, J.O.; Musetti, H.C.; Manzoli, A.; Zenatti, A.; Escote, M.T. Faujasite zeolite decorated with cobalt ferrite nanoparticles for improving removal and reuse in  $\text{Pb}^{2+}$  ions adsorption. *Chin. J. Chem. Eng.* **2020**, *28*, 1884–1890. [\[CrossRef\]](#)
69. Tabatabaefar, A.; Keshtkar, A.R.; Talebi, M.; Abolghasemi, H. Polyvinyl alcohol/alginate/zeolite nanohybrid for removal of metals. *Chem. Eng. Technol.* **2020**, *43*, 343–354. [\[CrossRef\]](#)
70. Abdelrahman, E.A.; El-Reash, Y.G.A.; Youssef, H.M.; Kotp, Y.H.; Hegazey, R.M. Utilization of rice husk and waste aluminum cans for the synthesis of some nanosized zeolite, zeolite/zeolite, and geopolymer/zeolite products for the efficient removal of Co (II), Cu (II), and Zn (II) ions from aqueous media. *J. Hazard. Mater.* **2021**, *401*, 123813. [\[CrossRef\]](#)
71. Shariatnia, Z.; Bagherpour, A. Synthesis of zeolite NaY and its nanocomposites with chitosan as adsorbents for lead(II) removal from aqueous solution. *Powder Technol.* **2018**, *338*, 744–763. [\[CrossRef\]](#)



72. Ghanavati, L.; Hekmati, A.H.; Rashidi, A.; Shafiekhani, A. Application of electrospun polyamide-6/modified zeolite nanofibrous composite to remove acid blue 74 dye from textile dyeing wastewater. *J. Text. Inst.* **2020**, *112*, 1730–1742. [\[CrossRef\]](#)
73. Pizarro, C.; Rubio, M.A.; Escudey, M.; Alborno, M.F.; Muñoz, D.; Denardin, J.; Fabris, J.D. Nanomagnetite-zeolite composites in the removal of arsenate from aqueous systems. *J. Braz. Chem. Soc.* **2015**, *26*, 1887–1896. [\[CrossRef\]](#)
74. Shafiee, M.; Abedi, M.A.; Abbasizadeh, S.; Sheshdeh, R.K.; Mousavi, S.E.; Shohani, S. Effect of zeolite hydroxyl active site distribution on adsorption of Pb (II) and Ni (II) pollutants from water system by polymeric nanofibers. *Sep. Sci. Technol.* **2020**, *55*, 1994–2011. [\[CrossRef\]](#)
75. Rad, L.R.; Momeni, A.; Ghazani, B.F.; Irani, M.; Mahmoudi, M.; Nogreh, B. Removal of Ni<sup>2+</sup> and Cd<sup>2+</sup> ions from aqueous solutions using electrospun PVA/zeolite nanofibrous adsorbent. *Chem. Eng. J.* **2014**, *256*, 119–127. [\[CrossRef\]](#)
76. Isawi, H. Using zeolite/polyvinyl alcohol/sodium alginate nanocomposite beads for removal of some heavy metals from wastewater. *Arab. J. Chem.* **2020**, *13*, 5691–5716. [\[CrossRef\]](#)
77. Abdelrahman, E.A. Synthesis of zeolite nanostructures from waste aluminum cans for efficient removal of malachite green dye from aqueous media. *J. Mol. Liq.* **2018**, *253*, 72–82. [\[CrossRef\]](#)
78. Abdelrahman, E.A.; Hegazy, R.M.; Alharbi, A. Facile synthesis of mordenite nanoparticles for efficient removal of Pb(II) ions from aqueous media. *J. Inorg. Organomet. Polym. Mater.* **2020**, *30*, 1369–1383. [\[CrossRef\]](#)
79. Borandegi, M.; Nezamzadeh-Ejhi, A. Enhanced removal efficiency of clinoptilolite nano-particles toward Co(II) from aqueous solution by modification with glutamic acid. *Colloids Surf. A Physicochem. Eng. Asp.* **2015**, *479*, 35–45. [\[CrossRef\]](#)
80. Heidari-Chaleshtori, M.; Nezamzadeh-Ejhi, A. Clinoptilolite nano-particles modified with aspartic acid for removal of Cu(II) from aqueous solutions: Isotherms and kinetic aspects. *New J. Chem.* **2015**, *39*, 9396–9406. [\[CrossRef\]](#)
81. Fakari, S.; Nezamzadeh-Ejhi, A. Synergistic effects of ion exchange and complexation processes in cysteine-modified clinoptilolite nanoparticles for removal of Cu(II) from aqueous solutions in batch and continuous flow systems. *New J. Chem.* **2017**, *41*, 3811–3820. [\[CrossRef\]](#)
82. Mehrali-Afjani, M.; Nezamzadeh-Ejhi, A. Efficient solid amino acid-clinoptilolite nanoparticles adsorbent for Mn(II) removal: A comprehensive study on designing the experiments, thermodynamic and kinetic aspects. *Solid State Sci.* **2020**, *101*, 106124. [\[CrossRef\]](#)
83. Nezamzadeh-Ejhi, A.; Kabiri-Samani, M. Effective removal of Ni(II) from aqueous solutions by modification of nano particles of clinoptilolite with dimethylglyoxime. *J. Hazard. Mater.* **2013**, *260*, 339–349. [\[CrossRef\]](#)
84. Shafiof, M.S.; Nezamzadeh-Ejhi, A. A comprehensive study on the removal of Cd(II) from aqueous solution on a novel pentetic acid-clinoptilolite nanoparticles adsorbent: Experimental design, kinetic and thermodynamic aspects. *Solid State Sci.* **2020**, *99*, 106071. [\[CrossRef\]](#)
85. Shakur, H.R.; Saraee, K.R.E.; Abdi, M.R.; Azimi, G. A novel PAN/NaX/ZnO nanocomposite absorbent: Synthesis, characterization, removal of uranium anionic species from contaminated water. *J. Mater. Sci.* **2016**, *51*, 9991–10004. [\[CrossRef\]](#)
86. Chen, J.; Gao, Q.; Zhang, X.; Liu, Y.; Wang, P.; Jiao, Y.; Yang, Y. Nanometer mixed-valence silver oxide enhancing adsorption of ZIF-8 for removal of iodide in solution. *Sci. Total Environ.* **2019**, *646*, 634–644. [\[CrossRef\]](#)
87. Shakur, H.R.; Saraee, K.R.E.; Abdi, M.R.; Azimi, G. Selective removal of uranium ions from contaminated waters using modified-X nanozeolite. *Appl. Rad. Isot.* **2016**, *118*, 43–55. [\[CrossRef\]](#)
88. Gasser, M.S.; Mekhamer, H.S.; Abdel Rahman, R.O. Optimization of the utilization of Mg/Fe hydrotalcite like Compounds in the removal of Sr(II) from aqueous solution. *J. Environ. Chem. Eng.* **2016**, *4*, 4619–4630. [\[CrossRef\]](#)
89. Gasser, M.S.; El Sherif, E.; Abdel Rahman, R.O. Modification of Mg-Fe hydrotalcite using Cyanex 272 for lanthanides separation. *Chem. Eng. J.* **2017**, *316C*, 758–769. [\[CrossRef\]](#)
90. Gasser, M.S.; El Sherif, E.; Mekhamer, H.S.; Abdel Rahman, R.O. Assessment of Cyanex 301 impregnated resin for its potential use to remove cobalt from aqueous solutions. *Environ. Res.* **2020**, *185*, 109402. [\[CrossRef\]](#) [\[PubMed\]](#)
91. Phillip, E.; Khoo, K.S.; Yusof, M.A.W.; Abdel Rahman, R.O. Assessment of POFA-cementitious material as backfill barrier in DSRS borehole disposal: <sup>226</sup>Ra confinement. *J. Environ. Manag.* **2021**, *280*, 111703. [\[CrossRef\]](#) [\[PubMed\]](#)
92. Ibrahim, H.A.; Abdel Moamen, O.A.; Monem, N.A.; Ismail, I.M. Assessment of kinetic and isotherm models for competitive sorption of Cs<sup>+</sup> and Sr<sup>2+</sup> from binary metal solution onto nanosized zeolite. *Chem. Eng. Commun.* **2018**, *205*, 1274–1287. [\[CrossRef\]](#)
93. Hassan, H.S.; Abdel Moamen, O.A.; Zaher, W.F. Adaptive Neuro-Fuzzy inference system analysis on sorption studies of strontium and cesium cations onto a novel impregnated nano-zeolite. *Adv. Powder Technol.* **2020**, *31*, 1125–1139. [\[CrossRef\]](#)
94. Abdel Moamen, O.A.; Hassan, H.S.; Zaher, W.F. Taguchi L16 optimization approach for simultaneous removal of Cs<sup>+</sup> and Sr<sup>2+</sup> ions by a novel scavenger. *Ecotoxicol. Environ. Saf.* **2020**, *189*, 110013. [\[CrossRef\]](#)
95. Barczyk, K.; Mozgawa, W.; Król, M. Studies of anions sorption on natural zeolites. *Spectrochim. Acta A Mol. Biomol. Spectrosc.* **2014**, *133*, 876–882. [\[CrossRef\]](#)
96. Filippidis, A.; Godelitsas, A.; Charistos, D.; Misaelides, P.; Kassoli-Fournaraki, A. The chemical behavior of natural zeolites in aqueous environments: Interactions between low-silica zeolites and 1 M NaCl solutions of different initial pH-values. *Appl. Clay Sci.* **1996**, *11*, 199–209. [\[CrossRef\]](#)
97. Chutia, P.; Kato, S.; Kojima, T.; Satokawa, S. Adsorption of As(V) on surfactant-modified natural zeolites. *J. Hazard. Mater.* **2009**, *162*, 204–211. [\[CrossRef\]](#)
98. De Gennaro, B.; Catalanotti, L.; Bowman, R.S.; Mercurio, M. Anion exchange selectivity of surfactant modified clinoptilolite-rich tuff for environmental remediation. *J. Colloid Interface Sci.* **2014**, *430*, 178–183. [\[CrossRef\]](#)



99. Li, Z. Influence of Solution pH and Ionic Strength on Chromate Uptake by Surfactant-Modified Zeolite. *J. Environ. Eng.* **2004**, *130*, 205–208. [\[CrossRef\]](#)
100. Leyva-Ramos, R.; Jacobo-Azuara, A.; Diaz-Flores, P.E.; Guerrero-Coronado, R.M.; Mendoza-Barron, J.; BerberMendoza, M.S. Adsorption of chromium(VI) from an aqueous solution on a surfactant-modified zeolite. *Colloids Surf. A Physicochem. Eng. Asp.* **2008**, *330*, 35–41. [\[CrossRef\]](#)
101. Mendoza-Barrón, J.; Jacobo-Azuara, A.; Leyva-Ramos, R.; Berber-Mendoza, M.S.; Guerrero-Coronado, R.M.; Fuentes-Rubio, L.; Martínez-Rosales, J.M. Adsorption of arsenic (V) from a water solution onto a surfactant-modified zeolite. *Adsorption* **2010**, *17*, 489–496. [\[CrossRef\]](#)
102. Haggerty, G.M.; Bowman, R.S. Sorption of chromate and other inorganic anions by organo-zeolite. *Environ. Sci. Technol.* **1994**, *28*, 452–458. [\[CrossRef\]](#) [\[PubMed\]](#)
103. Ghadiri, S.K.; Nabizadeh, R.; Mahvi, A.H.; Nasser, S.; Kazemian, H.; Mesdaghinia, A.R.; Nazmara, S. Methyl tert-butyl ether adsorption on surfactant modified natural zeolites. *Iran. J. Environ. Health Sci. Eng.* **2010**, *7*, 241–252.
104. Armağan, B.; Turan, M.; Elik, M.S. Equilibrium studies on the adsorption of reactive azo dyes into zeolite. *Desalination* **2004**, *170*, 33–39. [\[CrossRef\]](#)
105. Gómez-Hortigüela, L.; Pérez-Pariente, J.; García, R.; Chebude, Y.; Díaz, I. Natural zeolites from Ethiopia for elimination of fluoride from drinking water. *Sep. Purif. Technol.* **2013**, *120*, 224–229. [\[CrossRef\]](#)
106. Gómez-Hortigüela, L.; Pinar, A.B.; Pérez-Pariente, J.; Sani, T.; Chebude, Y.; Díaz, I. Ion-exchange in natural zeolite stilbite and significance in defluoridation ability. *Microporous Mesoporous Mater.* **2014**, *193*, 93–102. [\[CrossRef\]](#)
107. Adem, M.; Sani, T.; Chebude, Y.; Fetter, G.; Bosch, P.; Diaz, I. Comparison of the defluoridation capacity of zeolites from Ethiopia and Mexico. *Bull. Chem. Soc. Ethiop.* **2015**, *29*, 53. [\[CrossRef\]](#)
108. Cai, Q.; Turner, B.D.; Sheng, D.; Sloan, S. The kinetics of fluoride sorption by zeolite: Effects of cadmium, barium and manganese. *J. Contam. Hydrol.* **2015**, *177*, 177–178, 136–147. [\[CrossRef\]](#) [\[PubMed\]](#)
109. Sun, Y.; Fang, Q.; Dong, J.; Cheng, X.; Xu, J. Removal of fluoride from drinking water by natural stilbite zeolite modified with Fe(III). *Desalination* **2011**, *277*, 121–127. [\[CrossRef\]](#)
110. Velazquez-Peña, G.C.; Solache-Ríos, M.; Martínez-Miranda, V. Competing Effects of Chloride, Nitrate, and Sulfate Ions on the Removal of Fluoride by a Modified Zeolitic Tuff. *Water Air Soil Pollut.* **2014**, *226*, 2236. [\[CrossRef\]](#)
111. Zhang, Z.; Tan, Y.; Zhong, M. Defluorination of wastewater by calcium chloride modified natural zeolite. *Desalination* **2011**, *276*, 246–252. [\[CrossRef\]](#)
112. Peng, S.; Zeng, Q.; Guo, Y.; Niu, B.; Zhang, X.; Hong, S. Defluoridation from aqueous solution by chitosan modified natural zeolite. *J. Chem. Technol. Biotechnol.* **2013**, *88*, 1707–1714. [\[CrossRef\]](#)
113. Breck, D.W. Zeolite Molecular Sieves: Structure, Chemistry and Use. *Anal. Chim. Acta* **1975**, *75*, 493. [\[CrossRef\]](#)
114. Kosmulski, M. *Surface Charging and Points of Zero Charge*; CRC Press: Boca Raton, FL, USA, 2009.
115. Rožić, M.; Šipušić, Đ.I.; Sekovanić, L.; Miljanić, S.; Ćurković, L.; Hrenović, J. Sorption phenomena of modification of clinoptilolite tuffs by surfactant cations. *J. Colloid Interface Sci.* **2009**, *331*, 295–301. [\[CrossRef\]](#)
116. Li, Z. Sorption Kinetics of Hexadecyltrimethylammonium on Natural Clinoptilolite. *Langmuir* **1999**, *15*, 6438–6445. [\[CrossRef\]](#)
117. Ghomashi, P.; Charkhi, A.; Kazemini, M.; Yousefi, T. Removal of Fluoride from Wastewater by Natural and Modified Nano Clinoptilolite Zeolite. *J. Water Environ. Nanotechnol.* **2020**, *5*, 270–282.
118. Shevade, S.; Ford, R.G. Use of synthetic zeolites for arsenate removal from pollutant water. *Water Res.* **2004**, *38*, 3197–3204. [\[CrossRef\]](#) [\[PubMed\]](#)
119. Ragnarsdóttir, K.V. Dissolution kinetics of heulandite at pH 2–12 and 25 °C. *Geochem. Cosmochim. Acta* **1993**, *57*, 2439–2449. [\[CrossRef\]](#)
120. Gilani, N.S.; Tilami, S.E.; Azizi, S.N. One-step green synthesis of nano-sodalite zeolite and its performance for the adsorptive removal of crystal violet. *J. Chin. Chem. Soc.* **2021**, *68*, 2264–2273. [\[CrossRef\]](#)
121. Yürekli, Y. Determination of adsorption capacities of NaX Nano-particles against heavy metals and dyestuff. *J. Fac. Eng. Archit. Gaz.* **2019**, *34*, 2113–2124.
122. Nassara, M.Y.; Abdelrahman, E.A.; Aly, A.A.; Mohamed, T.Y. A facile synthesis of mordenite zeolite nanostructures for efficient bleaching of crude soybean oil and removal of methylene blue dye from aqueous media. *J. Mol. Liq.* **2017**, *248*, 302–313. [\[CrossRef\]](#)
123. Goyal, N.; Barman, S.; Bulasara, V.K. Efficient removal of bisphenol S from aqueous solution by synthesized nano-zeolite secony mobil-5. *Microporous Mesoporous Mater.* **2018**, *259*, 184–194. [\[CrossRef\]](#)
124. Ghifari, M.A.; Nuraini, A.; Permatasari, D.; Kamila, N.; Imanullah, T.; Astuti, Y. Nano-Zeolite Modification Using Cetylpyridinium Bromide for the Removal of Remazol Black B and Remazol Yellow G Dyes. *Adv. Sci. Lett.* **2017**, *23*, 6502–6505. [\[CrossRef\]](#)
125. Hassaninejad-Darzi, S.K.; Kavyani, S.; Torkamanzadeh, M.; Tilaki, R.D. Applicability of ZSM-5 nanozeolite to removal of ternary basic dyes: An adsorption study using high-accuracy UV/Vis-chemometric methods. *Monatsh. Chem.* **2017**, *148*, 2037–2049. [\[CrossRef\]](#)
126. Sivalingam, S.; Sen, S. Efficient removal of textile dye using nanosized fly ash derived zeolite-x: Kinetics and process optimization study. *J. Taiwan Inst. Chem. Eng.* **2019**, *96*, 305–314. [\[CrossRef\]](#)
127. Sarabadan, M.; Bashiri, H.; Mousavi, S.M. Adsorption of crystal violet dye by a zeolite-montmorillonite nano-adsorbent: Modelling, kinetic and equilibrium studies. *Clay Miner.* **2019**, *54*, 357–368. [\[CrossRef\]](#)

128. Robles-Mora, G.; Barrera-Cortés, J.; Valdez-Castro, L.; Solorza-Feria, O.; García-Díaz, C. Polycyclic Aromatic Hydrocarbon Sorption by Functionalized Humic Acids Immobilized in Micro- and Nano-Zeolites. *Sustainability* **2021**, *13*, 10391. [\[CrossRef\]](#)
129. Hu, G.; Yang, J.; Duan, X.; Farnood, R.; Yang, C.; Yang, J.; Liu, W.; Liu, Q. Recent developments and challenges in zeolite-based composite photocatalysts for environmental applications. *Chem. Eng. J.* **2021**, *417*, 129209. [\[CrossRef\]](#)
130. Miklos, D.B.; Remy, C.; Jekel, M.; Linden, K.G.; Drewes, J.E.; Hübner, U. Evaluation of advanced oxidation processes for water and wastewater treatment—A critical review. *Water Res.* **2018**, *139*, 118–131. [\[CrossRef\]](#) [\[PubMed\]](#)
131. Marcelo, C.R.; Puiatti, G.A.; Nascimento, M.A.; Oliveira, A.F.; Lopes, R.P. Degradation of the Reactive Blue 4 Dye in Aqueous Solution Using Zero-Valent Copper Nanoparticles. *J. Nanomater.* **2018**, *2018*, 4642038. [\[CrossRef\]](#)
132. Sun, S.; Xiao, W.; You, C.; Zhou, W.; Garba, Z.N.; Wang, L.; Yuan, Z. Methods for preparing and enhancing photocatalytic activity of basic bismuth nitrate. *J. Clean. Prod.* **2021**, *294*, 126350. [\[CrossRef\]](#)
133. Viter, R.; Iatsunskyi, I. Optical Spectroscopy for Characterization of Metal Oxide Nanofibers. In *Handbook of Nanofibers*; Barhoum, A., Bechelany, M., Makhoulouf, A., Eds.; Springer Nature: Cham, Switzerland, 2019.
134. Irshad, M.A.; Nawaz, R.; ur Rehman, M.Z.; Adrees, M.; Rizwan, M.; Ali, S.; Ahmad, S.; Tasleem, S. Synthesis, characterization and advanced sustainable applications of titanium dioxide nanoparticles: A review. *Ecotoxicol. Environm. Saf.* **2021**, *212*, 111978. [\[CrossRef\]](#)
135. Anandan, S.; Yoon, M. Photocatalytic activities of the nano-sized TiO<sub>2</sub>-supported Y-zeolites. *J. Photochem. Photobiol. C* **2003**, *4*, 5–18. [\[CrossRef\]](#)
136. Fonseca-Cervantes, O.R.; Pérez-Larios, A.; Arellano, V.H.R.; Sulbaran-Rangel, B.; Guzmán González, C.A. Effects in Band Gap for Photocatalysis in TiO<sub>2</sub> Support by Adding Gold and Ruthenium. *Processes* **2020**, *8*, 1032. [\[CrossRef\]](#)
137. Velásquez, J.; Valencia, S.; Rios, L.; Restrepo, G.; Marín, J. Characterization and photocatalytic evaluation of polypropylene and polyethylene pellets coated with P25 TiO<sub>2</sub> using the controlled-temperature embedding method. *Chem. Eng. J.* **2012**, *203*, 398–405. [\[CrossRef\]](#)
138. Šuligoj, A.; Pavlović, J.; Arčon, I.; Rajić, N.; Tušar, N.N. SnO<sub>2</sub>-Containing Clinoptilolite as a Composite Photocatalyst for Dyes Removal from Wastewater under Solar Light. *Catalysts* **2020**, *10*, 253. [\[CrossRef\]](#)
139. Zou, W.; Gao, B.; Ok, Y.S.; Dong, L. Integrated adsorption and photocatalytic degradation of volatile organic compounds (VOCs) using carbon-based nanocomposites: A critical review. *Chemosphere* **2019**, *218*, 845–859. [\[CrossRef\]](#) [\[PubMed\]](#)
140. Valente, J.P.S.; Padilha, P.M.; Florentino, A.O. Studies on the adsorption and kinetics of photodegradation of a model compound for heterogeneous photocatalysis onto TiO<sub>2</sub>. *Chemosphere* **2006**, *64*, 1128–1133. [\[CrossRef\]](#) [\[PubMed\]](#)
141. Armenise, S.; Garcia-Bordeje, E.; Valverde, J.L.; Romeo, E.; Monzón, A. A Langmuir–Hinshelwood approach to the kinetic modelling of catalytic ammonia decomposition in an integral reactor. *Phys. Chem. Chem. Phys.* **2013**, *15*, 12104–12117. [\[CrossRef\]](#)
142. Chekema, C.T.; Goetza, V.; Richardson, Y.; Plantarda, G.; Blinc, J. Modelling of adsorption/photodegradation phenomena on AC-TiO<sub>2</sub> composite catalysts for water treatment detoxification. *Catal. Today* **2019**, *328*, 183–188. [\[CrossRef\]](#)
143. Giovannetti, R.; Rommozzi, E.; D’Amato, C.A.; Zannotti, M. Kinetic Model for Simultaneous Adsorption/Photodegradation Process of Alizarin Red S in Water Solution by Nano-TiO<sub>2</sub> under Visible Light. *Catalysts* **2016**, *6*, 84. [\[CrossRef\]](#)
144. Sun, P.; Zhang, J.; Liu, W.; Wang, Q.; Cao, W. Modification to L-H Kinetics Model and Its Application in the Investigation on Photodegradation of Gaseous Benzene by Nitrogen-Doped TiO<sub>2</sub>. *Catalysts* **2018**, *8*, 326. [\[CrossRef\]](#)
145. Ali, M.H.H.; Goher, M.E.; Al-Afify, A.D.G. Kinetics and Adsorption Isotherm Studies of Methylene Blue Photodegradation Under UV Irradiation Using reduced Graphene Oxide-TiO<sub>2</sub> Nanocomposite in Different Wastewaters Effluents. *Egypt. J. Aquat. Biol. Fish.* **2019**, *23*, 253–263. [\[CrossRef\]](#)
146. Kakhki, R.M.; Karimian, A.; Hasan-nejad, H.; Ahsani, F. Zinc Oxide–Nanoclinoptilolite as a Superior Catalyst for Visible Photo-Oxidation of Dyes and Green Synthesis of Pyrazole Derivatives. *J. Inorg. Organomet. Polym. Mater* **2019**, *29*, 1358–1367. [\[CrossRef\]](#)
147. Li, H.; Zhang, Y.; Diao, J.; Qiang, M.; Chen, Z. Synthesis and Photocatalytic Activity of Hierarchical Zn-ZSM-5 Structures. *Catalysts* **2021**, *11*, 797. [\[CrossRef\]](#)
148. Nezamzadeh-Ejhieh, A.; Shirzadi, A. Enhancement of the photocatalytic activity of Ferrous Oxide by doping onto the nano-clinoptilolite particles towards photodegradation of tetracycline. *Chemosphere* **2014**, *107*, 136–144. [\[CrossRef\]](#)
149. Pourtaheri, A.; Nezamzadeh-Ejhieh, A. Enhancement in photocatalytic activity of NiO by supporting onto an Iranian clinoptilolite nano-particles of aqueous solution of cefuroxime pharmaceutical capsule. *Spectrochim. Acta A Mol. Biomol. Spectrosc.* **2015**, *137*, 338–344. [\[CrossRef\]](#)
150. Bahrami, M.; Nezamzadeh-Ejhieh, A. Effect of supporting and hybridizing of FeO and ZnO semiconductors onto an Iranian clinoptilolite nano-particles and the effect of ZnO/FeO ratio in the solar photodegradation of fish ponds waste water. *Mater. Sci. Semicond. Process.* **2014**, *27*, 833–840. [\[CrossRef\]](#)
151. Babaahamdi-Milani, M.; Nezamzadeh-Ejhieh, A. A comprehensive study on photocatalytic activity of supported Ni/Pb sulfide and oxide systems onto natural zeolite nanoparticles. *J. Hazard. Mater.* **2016**, *318*, 291–301. [\[CrossRef\]](#) [\[PubMed\]](#)
152. Nezamzadeh-Ejhieh, A.; Zabihi-Mobarakeh, H. Heterogeneous photodecolorization of mixture of methylene blue and bromophenol blue using CuO-nano-clinoptilolite. *J. Ind. Eng. Chem.* **2014**, *20*, 1421–1431. [\[CrossRef\]](#)
153. Derikvandi, H.; Nezamzadeh-Ejhieh, A. Comprehensive study on enhanced photocatalytic activity of heterojunction ZnS-NiS/zeolite nanoparticles: Experimental design based on response surface methodology (RSM), impedance spectroscopy and GC-MASS studies. *J. Colloid Interface Sci.* **2017**, *490*, 652–664. [\[CrossRef\]](#)

154. Esmaili-Hafshejani, J.; Nezamzadeh-Ejehieh, A. Increased photocatalytic activity of Zn(II)/Cu(II) oxides and sulfides by coupling and supporting them onto clinoptilolite nanoparticles in the degradation of benzophenone aqueous solution. *J. Hazard. Mater.* **2016**, *316*, 194–203. [[CrossRef](#)] [[PubMed](#)]
155. He, Z.; Lyu, Z.; Gu, Q.; Zhang, L.; Wang, J. Ceramic-based membranes for water and wastewater treatment. *Colloids Surf. A* **2019**, *578*, 123513. [[CrossRef](#)]
156. Far, R.M.; Van der Bruggen, B.; Verliefde, A.; Cornelissen, E. A review of zeolite materials used in membranes for water purification: History, applications, challenges and future trends. *J. Chem. Technol. Biotechnol.* **2021**. [[CrossRef](#)]
157. Sarkar, S.; Chakraborty, S. Nanocomposite polymeric membrane a new trend of water and wastewater treatment: A short review. *Groundw. Sustain. Dev.* **2021**, *12*, 100533. [[CrossRef](#)]
158. Ismail, A.F.; Padaki, M.; Hilal, N.; Matsuura, T.; Lau, W.J. Thin film composite membrane—Recent development and future potential. *Desalination* **2015**, *356*, 140–148. [[CrossRef](#)]
159. Adam, M.R.; Othman, M.H.D.; Samah, R.A.; Puteh, M.H.; Ismail, A.F.; Mustafa, A.; Rahman, M.A.; Jaafar, J. Current trends and future prospects of ammonia removal in wastewater: A comprehensive review on adsorptive membrane development. *Sep. Purif. Technol.* **2019**, *213*, 114. [[CrossRef](#)]
160. Kim, S.; Nam, S.N.; Jang, A.; Jang, M.; Park, C.M.; Son, A.; Her, N.; Heo, J.; Yoon, Y. Review of adsorption–membrane hybrid systems for water and wastewater treatment. *Chemosphere* **2022**, *286*, 131916. [[CrossRef](#)]
161. Cui, J.; Li, F.; Wang, Y.; Zhang, Q.; Ma, W.; Huang, C. Electrospun nanofiber membranes for wastewater treatment applications. *Sep. Purif. Technol.* **2020**, *250*, 117116. [[CrossRef](#)]
162. Habiba, U.; Siddique, T.A.; Lee, J.J.L.; Joo, T.C.; Ang, B.C.; Afifi, A.M. Adsorption study of methyl orange by chitosan/polyvinyl alcohol/zeolite electrospun composite nanofibrous membrane. *Carbohydr. Polym.* **2018**, *191*, 79–85. [[CrossRef](#)] [[PubMed](#)]
163. Habiba, U.; Afifi, A.M.; Salleh, A.; Ang, B.C. Chitosan/(polyvinyl alcohol)/zeolite electrospun composite nanofibrous membrane for adsorption of  $\text{Cr}^{6+}$ ,  $\text{Fe}^{3+}$  and  $\text{Ni}^{2+}$ . *J. Hazard. Mater.* **2017**, *322*, 182–194. [[CrossRef](#)] [[PubMed](#)]
164. Saranya, R.; Arthanareeswaran, G.; Ismail, A.F. Enhancement of anti-fouling properties during the treatment of paper mill effluent using functionalized zeolite and activated carbon nanomaterials based ultrafiltration. *J. Chem. Technol. Biotechnol.* **2019**, *94*, 2805–2815. [[CrossRef](#)]
165. Anis, S.F.; Lalia, B.S.; Lesimple, A.; Hashaiekh, R.; Hilal, N. Electrically conductive membranes for contemporaneous dye rejection and degradation. *Chem. Eng. J.* **2022**, *428*, 131184. [[CrossRef](#)]
166. Sultana, N.; Rahman, R. Electrospun nanofiber composite membranes based on cellulose acetate/nano-zeolite for the removal of oil from oily wastewater. *Emerg. Mater.* **2021**. [[CrossRef](#)]
167. Moghimifar, V.; Livari, A.E.; Raisi, A.; Aroujalian, A. Enhancing the antifouling property of polyethersulfone ultrafiltration membranes using NaX zeolite and titanium oxide nanoparticles. *RSC Adv.* **2015**, *5*, 55964–55976. [[CrossRef](#)]
168. Esmaeili, A.; Saremnia, B. Comparison study of adsorption and nanofiltration methods for removal of total petroleum hydrocarbons from oil-field wastewater. *J. Pet. Sci. Eng.* **2018**, *171*, 403–413. [[CrossRef](#)]
169. Yu, C.; Wu, J.; Zin, G.; Di Luccio, M.; Wen, D.; Qilin, L. D-Tyrosine loaded nanocomposite membranes for environmental-friendly, long-term biofouling control. *Water Res.* **2018**, *30*, 105–114. [[CrossRef](#)]
170. Omer, A.M.; Dey, R.; Eltaweil, A.S.; Abd El-Monaem, E.M.; Ziora, Z.M. Insights into recent advances of chitosan-based adsorbents for sustainable removal of heavy metals and anions. *Arab. J. Chem.* **2022**, *15*, 103543. [[CrossRef](#)]
171. Yurekli, Y. Removal of heavy metals in wastewater by using zeolite nano-particles impregnated polysulfone membranes. *J. Hazard. Mater.* **2016**, *309*, 53–64. [[CrossRef](#)] [[PubMed](#)]